



Gradient Transformation Trajectory Following Algorithms for Equality-Constrained Minimization[†]

W. J. Grantham*

*School of Mechanical and Materials Engineering
Washington State University
Pullman, Washington 99164-2920
United States of America*

Received: November 15, 2009; Revised: March 25, 2010

Abstract: For minimizing a scalar-valued function subject to equality constraints, we develop and investigate a family of gradient transformation differential equation algorithms. This family includes, as special cases: Min-Max Ascent, Hestenes' Method of Multipliers, Newton's method, and a Gradient Enhanced Min-Max (GEMM) algorithm that we extend to handle equality constraints. We apply these methods to Rosenbrock's function with a parabolic constraint. We show that Min-Max Ascent is locally and (experimentally) globally asymptotically stable but extremely stiff and has extremely slow convergence. Hestenes' Method of Multipliers is also locally and (experimentally) globally asymptotically stable and has faster convergence, but is still very stiff. Newton's method is not stiff, but does not yield global asymptotic stability. However, GEMM is both globally asymptotically stable and not stiff. We study the stiffness of the gradient transformation family in terms of Lyapunov exponent time histories. Starting from points where all the methods in this paper do work, we show that Min-Max Ascent and Hestenes' Method of Multipliers are very stiff and slow to converge, but with the Method of Multipliers being approximately 2 times as fast as Min-Max Ascent. Newton's method is not stiff and is approximately 900 times as fast as Min-Max Ascent and 400 times as fast as the Method of Multipliers. In contrast, the Gradient Enhanced Min-Max method is globally convergent, is not stiff, and is approximately 100 times faster than Newton's method, 40,000 times faster than the Method of Multipliers, and 90,000 times faster than Min-Max Ascent.

Keywords: *nonlinear programming, Lagrangian Min-Max, stiff differential equations, Lyapunov exponents.*

Mathematics Subject Classification (2000): 90C30, 90C47, 70K70, 34D08.

[†] In Memoriam: Thomas Lange Vincent, Doctor of Philosophy, Professor Emeritus, The University of Arizona: Born, September 16, 1935; Died, October 26, 2009.

* Corresponding author: <mailto:grantham@wsu.edu>

1 Minimization with Equality Constraints

We consider the nonlinear programming problem of finding a point $\mathbf{x}^* \in \mathcal{R}^n$ to

$$\min \phi(\mathbf{x}) \quad \text{subject to} \quad \boldsymbol{\psi}(\mathbf{x}) = \mathbf{0}, \quad (1)$$

where the functions $\phi(\cdot) : \mathcal{R}^n \rightarrow \mathcal{R}^1$ and $\boldsymbol{\psi}(\cdot) : \mathcal{R}^n \rightarrow \mathcal{R}^m$ are \mathcal{C}^2 . We develop differential equation algorithms of the form

$$\dot{\mathbf{x}} = \mathbf{g}(\mathbf{x}),$$

where $(\dot{\cdot})$ denotes $d(\cdot)/dt$ and t is time. We choose the function $\mathbf{g}(\cdot)$ with the objective of having solutions $\mathbf{x}(t) \rightarrow \mathbf{x}^*$ as $t \rightarrow \infty$. Such “trajectory following” algorithms have received considerable attention in recent years. In [1] Steepest Descent differential equations are used to design controllers for nonlinear systems. In [2] optimal control differential equations are used to design new discrete minimization algorithms. In [3] and [4] differential equation algorithms are investigated for min-max optimization problems. In [5] and [6] differential equations for Newton’s method are used to find all of the stationary points of a function. In [7] a Gradient Enhanced Newton algorithm is developed for finding a stationary proper minimum point. In [8] a Gradient Enhanced Min-Max method is developed for finding a proper stationary min-max saddle point.

In this paper, we extend the stationary min and min-max results of [7] and [8] to include equality constraints. As in these previous papers, we are concerned with differential equation-based algorithms, and with the stiffness and domain of stability of a family of gradient-based numerical update algorithms. These algorithms include, as special cases, Steepest Descent, Min-Max Ascent, Newton’s Method, augmented Lagrangians and Hestenes’ Method of Multipliers, and the Gradient Enhanced Min-Max algorithm that we extend here for minimization subject to equality constraints. We use Lyapunov exponents to measure the stiffness (*e.g.*, widely separated time scales and eigenvalues) of the various algorithms when applied to an equality constrained version of Rosenbrock’s “banana” function.

2 Necessary Conditions at a Minimum Point

The necessary conditions for $\mathbf{x}^* \in \mathcal{R}^n$ to yield a regular [9, p. 35] local minimum can be expressed in terms of the Lagrangian

$$L(\mathbf{x}, \boldsymbol{\lambda}) \triangleq \phi(\mathbf{x}) - \boldsymbol{\lambda}^\top \boldsymbol{\psi}(\mathbf{x}), \quad (2)$$

where $\boldsymbol{\lambda} \in \mathcal{R}^m$ is a vector of Lagrange multipliers and $\boldsymbol{\psi}(\cdot) : \mathcal{R}^n \rightarrow \mathcal{R}^m$ represents a system of $m < n$ equality constraints that must be satisfied at \mathbf{x}^* .

The first-order Karush–Kuhn–Tucker necessary conditions [9, p.57] are that:

$$\mathbf{0}^\top = \frac{\partial L}{\partial \mathbf{x}} = \frac{\partial \phi}{\partial \mathbf{x}} - \boldsymbol{\lambda}^\top \frac{\partial \boldsymbol{\psi}}{\partial \mathbf{x}}, \quad \mathbf{0}^\top = \frac{\partial L}{\partial \boldsymbol{\lambda}} = -\boldsymbol{\psi}^\top(\mathbf{x}), \quad (3)$$

where $\partial L / \partial \mathbf{x} \triangleq [\partial L / \partial x_1, \dots, \partial L / \partial x_n]$. Since $\partial L / \partial \boldsymbol{\lambda} = -\boldsymbol{\psi}^\top$ the necessary conditions can be written in terms of $\mathbf{y}^\top = [\mathbf{x}^\top, \boldsymbol{\lambda}^\top] \in \mathcal{R}^p$, $p = n + m$, as

$$\nabla_{\mathbf{y}} L(\mathbf{y}) \triangleq \left[\frac{\partial L}{\partial \mathbf{y}} \right]^\top = \mathbf{0}, \quad (4)$$

that is,

$$\nabla_{\mathbf{x}}L = \left[\frac{\partial\phi}{\partial\mathbf{x}} \right]^T - \left[\frac{\partial\psi}{\partial\mathbf{x}} \right]^T \boldsymbol{\lambda} = \mathbf{0}, \quad \nabla_{\boldsymbol{\lambda}}L = \left[\frac{\partial L}{\partial\boldsymbol{\lambda}} \right]^T = -\boldsymbol{\psi} = \mathbf{0}.$$

The necessary conditions (4) are stationarity conditions, yielding candidates that may be local minima, maxima, or saddle points. Suppose that the constraint qualification conditions [9, p. 55] hold: that at \mathbf{x}^* there exists a nonzero vector $\boldsymbol{\eta} \in \mathcal{R}^n$ tangent to the constraints $\boldsymbol{\psi}(\mathbf{x}^*) = \mathbf{0}$. Then the second-order necessary condition [9, p. 56] for a regular local minimum point is that

$$\boldsymbol{\eta}^T H(\mathbf{x}^*, \boldsymbol{\lambda}^*) \boldsymbol{\eta} \geq 0 \quad \text{for all nonzero } \boldsymbol{\eta} \text{ such that } \frac{\partial\boldsymbol{\psi}(\mathbf{x}^*)}{\partial\mathbf{x}} \boldsymbol{\eta} = \mathbf{0}, \tag{5}$$

where $H(\mathbf{x}, \boldsymbol{\lambda}) = \partial^2 L(\mathbf{x}, \boldsymbol{\lambda}) / \partial \mathbf{x}^2$. A second-order sufficient condition is that $\nabla_{\mathbf{y}}L(\mathbf{y}) = [\partial L(\mathbf{y}^*) / \partial \mathbf{y}]^T = \mathbf{0}$ and

$$\boldsymbol{\eta}^T H(\mathbf{x}^*, \boldsymbol{\lambda}^*) \boldsymbol{\eta} > 0 \quad \text{for all nonzero } \boldsymbol{\eta} \text{ such that } \frac{\partial\boldsymbol{\psi}(\mathbf{x}^*)}{\partial\mathbf{x}} \boldsymbol{\eta} = \mathbf{0}, \tag{6}$$

which would be satisfied, for example, by the stronger condition that $H(\mathbf{x}^*, \boldsymbol{\lambda}^*)$ be positive definite.

3 Numerical Minimization Methods

Numerical minimization methods [10] generally seek a search direction \mathbf{s} and a step size α for a move $\mathbf{x} \leftarrow \mathbf{x} + \alpha\mathbf{s}$. Here, we focus on the instantaneous search direction, using a differential step size with continuous updating of the search direction. Thus we develop “trajectory following” algorithms of the form $d\mathbf{x}/dt = \mathbf{g}(\mathbf{x})$. Such differential equations-based algorithms have been very useful in developing new discrete optimization algorithms [2] based on long-term optimal control algorithms. In addition, using a differential step size avoids difficulties such as “chatter” that can occur with discrete step size algorithms such as Steepest Descent applied, for example, to Rosenbrock’s function [7].

3.1 Unconstrained minimization

3.1.1 Steepest descent

The simplest algorithm for minimizing an unconstrained function $\phi(\mathbf{x})$ is the Steepest Descent algorithm

$$\dot{\mathbf{x}} = -\nabla\phi,$$

with $\nabla\phi \triangleq [\partial\phi/\partial\mathbf{x}]^T$, which yields

$$\frac{d\phi}{dt} = \frac{\partial\phi}{\partial\mathbf{x}} \dot{\mathbf{x}} = -\|\nabla\phi\|^2,$$

where $\|\cdot\|$ denotes the Euclidian norm. If \mathbf{x}^* is a local minimal point for $\phi(\mathbf{x})$ then $V(\mathbf{x}) = \phi(\mathbf{x}) - \phi(\mathbf{x}^*)$ is a local Lyapunov function, establishing that Steepest Descent is at least locally asymptotically stable at a proper local minimum. In addition, if \mathbf{x}^* is unique and $\|\nabla\phi(\mathbf{x})\| \rightarrow \infty$ as $\|\mathbf{x}\| \rightarrow \infty$ then the minimal point \mathbf{x}^* is globally asymptotically stable.

Steepest Descent may produce stiff systems. Such systems require much more complicated differential equation solvers than Euler’s method or Runge–Kutta methods, leading to complicated discrete versions.

3.1.2 Newton's method

From Taylor's theorem applied to the stationarity necessary condition

$$\nabla\phi = \mathbf{0},$$

we get

$$\nabla\phi(\mathbf{x} + \Delta\mathbf{x}) = \nabla\phi(\mathbf{x}) + \nabla^2\phi(\mathbf{x})\Delta\mathbf{x} + O(\|\Delta\mathbf{x}\|^2), \quad (7)$$

where $\nabla^2\phi \triangleq \partial^2\phi/\partial\mathbf{x}^2$ is the Hessian matrix, $\Delta\mathbf{x} = \dot{\mathbf{x}}\Delta t + O(\Delta t^2)$, and $O(\alpha^2)/\alpha \rightarrow 0$ as $\alpha \rightarrow 0$. Setting the left-hand side equal to zero yields the discrete-time ($\Delta t = 1$, small $\|\Delta\mathbf{x}\|$) version of Newton's method: $\Delta\mathbf{x} = -[\nabla^2\phi]^{-1}\nabla\phi$.

In the limit as $\Delta t \rightarrow 0$, the continuous-time Newton method is given by

$$\dot{\mathbf{x}} = -[\nabla^2\phi]^{-1}\nabla\phi. \quad (8)$$

The discrete-time version of Newton's method corresponds to applying Euler integration $\Delta\mathbf{x} = \dot{\mathbf{x}}\Delta t$ to (8) with $\Delta t = 1$.

Note that Newton's method is only well defined in a region where the determinant $|\nabla^2\phi(\mathbf{x})|$ does not change sign and is nonzero, such as some neighborhood of a proper local minimal point \mathbf{x}^* , at which $\nabla^2\phi(\mathbf{x}^*) > 0$ (positive definite). Newton's method, in regions where it does work, typically converges much faster than Steepest Descent, and yields non-stiff systems. In particular, in terms of the gradient $\nabla\phi[\mathbf{x}(t)]$ along $\mathbf{x}(t)$, Newton's method (8) yields

$$\frac{d\nabla\phi}{dt} = [\nabla^2\phi]\dot{\mathbf{x}} = -\nabla\phi,$$

which is non stiff, with eigenvalues $\mu_k = -1$, $k = 1, \dots, n$. Note that, along $\mathbf{x}(t)$ we have $\nabla\phi[\mathbf{x}(t)] = \nabla\phi[\mathbf{x}(0)]e^{-t} \rightarrow \mathbf{0}$ as $t \rightarrow \infty$, hence $\nabla\phi[\mathbf{x}(t)] \rightarrow \mathbf{0}$. As with Steepest Descent, Newton's method is at least locally asymptotically stable to a proper local minimal point.

3.2 Constrained minimization

3.2.1 Penalty functions

The earliest approach to handling equality constraints $\boldsymbol{\psi}(\mathbf{x}) = \mathbf{0}$ was to apply unconstrained minimization to a penalty function such as Courant's penalty function

$$\pi(\mathbf{x}, \beta) = \phi(\mathbf{x}) + \frac{1}{2}\beta\|\boldsymbol{\psi}(\mathbf{x})\|^2 = \phi(\mathbf{x}) + \frac{1}{2}\beta\boldsymbol{\psi}^\top(\mathbf{x})\boldsymbol{\psi}(\mathbf{x}), \quad (9)$$

with a sequence of increasing values for $\beta > 0$. Then Steepest Descent yields

$$\dot{\mathbf{x}} = -\nabla\pi = -\nabla\phi(\mathbf{x}) - \beta\boldsymbol{\Gamma}^\top(\mathbf{x})\boldsymbol{\psi}(\mathbf{x}),$$

where $\boldsymbol{\Gamma} \in \mathcal{R}^{m \times n}$ is given by

$$\boldsymbol{\Gamma}(\mathbf{x}) = \partial\boldsymbol{\psi}(\mathbf{x})/\partial\mathbf{x}. \quad (10)$$

The main difficulty with this approach is that, for any finite $\beta > 0$, the point that minimizes $\pi(\mathbf{x}, \beta)$ is not exactly the same point that minimizes $\phi(\mathbf{x})$ subject to $\boldsymbol{\psi}(\mathbf{x}) = \mathbf{0}$, except in the limit as $\beta \rightarrow \infty$. In addition, large values of β yield stiff systems. Note that Newton's method applied to (9) may alleviate the stiffness, but not the "mismatch" between the two minimization solutions, which requires $\beta \rightarrow \infty$.

3.2.2 Newton’s method

The first-order necessary conditions for a stationary point of $\phi(\mathbf{x})$ subject to $\psi(\mathbf{x}) = \mathbf{0}$ are given by (3) in terms of a Lagrange multiplier vector. Newtons method, applied to (4), is given by

$$\begin{bmatrix} \dot{\mathbf{x}} \\ \dot{\boldsymbol{\lambda}} \end{bmatrix} = -\mathbf{H}^{-1}(\mathbf{y}) \begin{bmatrix} \nabla_{\mathbf{x}}L \\ -\psi(\mathbf{x}) \end{bmatrix}, \tag{11}$$

where

$$H(\mathbf{y}) = \nabla_{\mathbf{y}}^2 L \triangleq \frac{\partial^2 L}{\partial \mathbf{y}^2} = \begin{bmatrix} \frac{\partial^2 L}{\partial \mathbf{x}^2} & \frac{\partial^2 L}{\partial \boldsymbol{\lambda} \partial \mathbf{x}} \\ \frac{\partial^2 L}{\partial \mathbf{x} \partial \boldsymbol{\lambda}} & \frac{\partial^2 L}{\partial \boldsymbol{\lambda}^2} \end{bmatrix} = \begin{bmatrix} \frac{\partial^2 L}{\partial \mathbf{x}^2} & -\boldsymbol{\Gamma}^\top \\ -\boldsymbol{\Gamma} & \mathbf{0} \end{bmatrix}. \tag{12}$$

3.2.3 Min-Max Lagrangians

Consider the Lagrangian

$$L(\mathbf{x}, \boldsymbol{\lambda}) = \phi(\mathbf{x}) - \boldsymbol{\lambda}^\top \psi(\mathbf{x}).$$

Let $\mathbf{x}(\boldsymbol{\lambda})$ denote the unconstrained minimizer for $L(\mathbf{x}, \boldsymbol{\lambda})$, and let \mathbf{x}^* and $\boldsymbol{\lambda}^*$ be the solution and Lagrange multiplier, respectively, for the constrained minimization problem (1). Then $L(\mathbf{x}(\boldsymbol{\lambda}), \boldsymbol{\lambda}) \leq L(\mathbf{x}, \boldsymbol{\lambda}) \forall \mathbf{x}$, along with $\psi(\mathbf{x}^*) = \mathbf{0}$, yields

$$\begin{aligned} L(\mathbf{x}(\boldsymbol{\lambda}), \boldsymbol{\lambda}) &\leq L(\mathbf{x}^*, \boldsymbol{\lambda}) = \phi(\mathbf{x}^*) - \boldsymbol{\lambda}^\top \psi(\mathbf{x}^*) \\ &= \phi(\mathbf{x}^*) = \phi(\mathbf{x}^*) - \boldsymbol{\lambda}^{*\top} \psi(\mathbf{x}^*) \\ &= L(\mathbf{x}^*, \boldsymbol{\lambda}^*) = L(\mathbf{x}(\boldsymbol{\lambda}^*), \boldsymbol{\lambda}^*). \end{aligned}$$

Thus

$$L(\mathbf{x}^*, \boldsymbol{\lambda}^*) = \max_{\boldsymbol{\lambda}} \min_{\mathbf{x}} L(\mathbf{x}, \boldsymbol{\lambda}) = \min_{\mathbf{x}} \max_{\boldsymbol{\lambda}} L(\mathbf{x}, \boldsymbol{\lambda}), \tag{13}$$

since $L(\mathbf{x}, \boldsymbol{\lambda})$ is linear in $\boldsymbol{\lambda}$.

A Min-Max Ascent algorithm [3] for achieving the Lagrangian saddle point defined by (13) is given by

$$\dot{\mathbf{x}} = -\nabla_{\mathbf{x}}L(\mathbf{x}, \boldsymbol{\lambda}) = -\nabla\phi(\mathbf{x}) + \boldsymbol{\Gamma}^\top(\mathbf{x})\boldsymbol{\lambda}, \tag{14}$$

$$\dot{\boldsymbol{\lambda}} = \nabla_{\boldsymbol{\lambda}}L(\mathbf{x}, \boldsymbol{\lambda}) = -\psi(\mathbf{x}). \tag{15}$$

As noted in [11], methods such as this, where \mathbf{x}^* solves the primal problem (1) and $\boldsymbol{\lambda}(\mathbf{u})$ is the Lagrange multiplier vector for an associated dual problem [12, p. 113]:

$$\min_{\substack{\mathbf{u} \in \mathcal{N}_{\mathbf{u}} \\ \mathbf{x}(\mathbf{u}) \in \mathcal{N}_{\mathbf{x}}}} \phi[\mathbf{x}(\mathbf{u})] \quad \text{subject to} \quad \psi[\mathbf{x}(\mathbf{u})] = \mathbf{u} \tag{16}$$

with $\boldsymbol{\lambda}(\mathbf{0}) = \boldsymbol{\lambda}^*$ and $\mathcal{N}_{\mathbf{u}} \subset \mathcal{R}^m$ and $\mathcal{N}_{\mathbf{x}} \subset \mathcal{R}^n$ being small neighborhoods of $\mathbf{u}^* = \mathbf{0}$ and \mathbf{x}^* , respectively, have “... serious disadvantages. First, problem (1) must have a locally convex structure in order for the dual problem (16) to be well defined and (15) to be meaningful. Second, ..., the ascent iteration (15) converges only moderately fast.”

3.2.4 Augmented Lagrangians

The following results apply to the equality constrained problem (1), but can be extended to the general nonlinear programming problem with equality and inequality constraints.

Consider an augmented Lagrangian [13]

$$\mathcal{L}(\mathbf{x}, \boldsymbol{\lambda}, \boldsymbol{\beta}) \triangleq L(\mathbf{x}, \boldsymbol{\lambda}) + \frac{1}{2}\boldsymbol{\psi}(\mathbf{x})^\top \mathbf{S}\boldsymbol{\psi}(\mathbf{x}) = \phi(\mathbf{x}) + \frac{1}{2}\boldsymbol{\psi}(\mathbf{x})^\top \mathbf{S}\boldsymbol{\psi}(\mathbf{x}) - \boldsymbol{\lambda}^\top \boldsymbol{\psi}(\mathbf{x}), \quad (17)$$

where $\boldsymbol{\beta} \in \mathcal{R}^m$, $\boldsymbol{\beta} \geq \mathbf{0}$, and $\mathbf{S} = \text{diag}[\boldsymbol{\beta}] \in \mathcal{R}^{m \times m}$. The augmented Lagrangian (17) can be viewed either as 1) the Lagrangian plus a penalty term or 2) the Lagrangian for minimizing a weighted Courant penalty function (9) subject to $\boldsymbol{\psi}(\mathbf{x}) = \mathbf{0}$. In the first case view, since a purely \mathbf{x} -dependent penalty term has been added to $L(\mathbf{x}, \boldsymbol{\lambda})$, we expect that in changing to a $\max_{\boldsymbol{\lambda}} \min_{\mathbf{x}} \mathcal{L}(\mathbf{x}, \boldsymbol{\lambda})$ vs. $\max_{\boldsymbol{\lambda}} \min_{\mathbf{x}} L(\mathbf{x}, \boldsymbol{\lambda})$ process, $\boldsymbol{\lambda}$ has no effect, but \mathbf{x} affords a trade-off between the \mathbf{x} that minimizes $L(\mathbf{x}, \boldsymbol{\lambda})$ and the \mathbf{x} that minimizes $\mathcal{L}(\mathbf{x}, \boldsymbol{\lambda}, \boldsymbol{\beta})$. However, the penalty weights β_i on the ψ_i do not need to approach infinity for the two solutions to be the same and can be quite moderate in size. We have:

Theorem 3.1 *If second-order sufficient conditions (6) hold at $(\mathbf{x}^*, \boldsymbol{\lambda}^*)$ then there exists $\boldsymbol{\beta}' \geq \mathbf{0}$ such that for any $\boldsymbol{\beta} > \boldsymbol{\beta}'$, \mathbf{x}^* is an isolated local minimizer of $\mathcal{L}(\mathbf{x}, \boldsymbol{\lambda}^*, \boldsymbol{\beta})$, that is, $\mathbf{x}^* = \mathbf{x}(\boldsymbol{\lambda}^*)$. Furthermore, $\boldsymbol{\lambda}^*$ is a local maximizer of $\nu(\boldsymbol{\lambda}) \triangleq \mathcal{L}(\mathbf{x}(\boldsymbol{\lambda}), \boldsymbol{\lambda}, \boldsymbol{\beta})$.*

Proof [10, pp. 289–291].

Hereafter we consider the case where $\mathbf{S} = \beta \mathbf{I}_m$ and drop the $\boldsymbol{\beta}$ argument in $\mathcal{L}(\cdot)$ unless it is expressly needed for the discussion.

4 Gradient Transformation Trajectory Following

From Theorem 3.1 we seek a $\max_{\boldsymbol{\lambda}} \min_{\mathbf{x}} \mathcal{L}(\mathbf{x}, \boldsymbol{\lambda})$. We consider the class of *Gradient Transformation algorithms*, of the form

$$\dot{\mathbf{y}} = -\mathbf{P}(\mathbf{y})\nabla_{\mathbf{y}}\mathcal{L}(\mathbf{y}), \quad (18)$$

where $\mathbf{P}(\mathbf{y}) \in \mathcal{R}^{p \times p}$ is a Gradient Transformation matrix to be chosen, $\mathbf{y} \in \mathcal{R}^p$ with $\mathbf{y}^\top = [\mathbf{x}^\top, \boldsymbol{\lambda}^\top]$, and

$$\mathbf{h}(\mathbf{y}) = \nabla_{\mathbf{y}}\mathcal{L}(\mathbf{y}) = \begin{bmatrix} \nabla_{\mathbf{x}}\mathcal{L} \\ \nabla_{\boldsymbol{\lambda}}\mathcal{L} \end{bmatrix} = \begin{bmatrix} \nabla_{\mathbf{x}}L + \beta\boldsymbol{\Gamma}^\top\boldsymbol{\psi} \\ \nabla_{\boldsymbol{\lambda}}L \end{bmatrix} = \begin{bmatrix} \nabla\phi - \boldsymbol{\Gamma}^\top[\boldsymbol{\lambda} - \beta\boldsymbol{\psi}] \\ -\boldsymbol{\psi} \end{bmatrix}. \quad (19)$$

Thus the Gradient Transformation algorithms are of the form

$$\begin{bmatrix} \dot{\mathbf{x}} \\ \dot{\boldsymbol{\lambda}} \end{bmatrix} = - \begin{bmatrix} \mathbf{P}_{\mathbf{xx}} & \mathbf{P}_{\mathbf{x}\boldsymbol{\lambda}} \\ \mathbf{P}_{\boldsymbol{\lambda}\mathbf{x}} & \mathbf{P}_{\boldsymbol{\lambda}\boldsymbol{\lambda}} \end{bmatrix} \begin{bmatrix} \nabla_{\mathbf{x}}\mathcal{L} \\ \nabla_{\boldsymbol{\lambda}}\mathcal{L} \end{bmatrix} = \begin{bmatrix} \mathbf{P}_{\mathbf{xx}} & \mathbf{P}_{\mathbf{x}\boldsymbol{\lambda}} \\ \mathbf{P}_{\boldsymbol{\lambda}\mathbf{x}} & \mathbf{P}_{\boldsymbol{\lambda}\boldsymbol{\lambda}} \end{bmatrix} \begin{bmatrix} -\nabla\phi + \boldsymbol{\Gamma}^\top[\boldsymbol{\lambda} - \beta\boldsymbol{\psi}] \\ \boldsymbol{\psi} \end{bmatrix}. \quad (20)$$

If $\mathbf{P}(\mathbf{y})$ is nonsingular in a region $\mathcal{R} \subseteq \mathcal{R}^p$ containing $\mathbf{y}^* = (\mathbf{x}^*, \boldsymbol{\lambda}^*)$ then for (18) the only equilibrium points in \mathcal{R} are where $\nabla_{\mathbf{y}}\mathcal{L}(\mathbf{y}^*) = \mathbf{0}$. We will be concerned with the uniqueness and local and global stability of the (possibly multiple) equilibria and with the “stiffness” of the resulting system, corresponding to various choices for $\mathbf{P}(\mathbf{y})$.

4.1 Min-Max ascent

The original trajectory following method [3] for seeking $\max_{\lambda} \min_{\mathbf{x}} \mathcal{L}(\mathbf{x}, \lambda)$ is via steepest descent for \mathbf{x} and steepest ascent for λ , yielding

$$\begin{aligned} \dot{\mathbf{x}} &= -\nabla_{\mathbf{x}}\mathcal{L} = -[\nabla_{\mathbf{x}}L + \beta\Gamma^T\psi] = -\nabla_{\mathbf{x}}\phi + \Gamma^T[\lambda - \beta\psi], \\ \dot{\lambda} &= \nabla_{\lambda}\mathcal{L} = \nabla_{\lambda}L = -\psi. \end{aligned}$$

This corresponds to choosing

$$\mathbf{P} = \begin{bmatrix} \mathbf{P}_{\mathbf{xx}} & \mathbf{P}_{\mathbf{x}\lambda} \\ \mathbf{P}_{\lambda\mathbf{x}} & \mathbf{P}_{\lambda\lambda} \end{bmatrix} = \begin{bmatrix} \mathbf{I}_n & \mathbf{0} \\ \mathbf{0} & -\mathbf{I}_m \end{bmatrix} \tag{21}$$

in (20), where \mathbf{I}_p denotes the $p \times p$ identity matrix.

4.2 Hestenes’ method of multipliers

In a discrete-time setting let λ_k denote the current estimate for the Lagrange multiplier λ^* and let $\mathbf{x} = \mathbf{x}(\lambda_k)$ denote the minimizer of $\mathcal{L}(\mathbf{x}, \lambda_k)$. Then

$$\mathbf{0} = \nabla_{\mathbf{x}}\mathcal{L} = \nabla_{\mathbf{x}}L + \beta\Gamma^T\psi = \nabla_{\mathbf{x}}\phi - \Gamma^T[\lambda_k - \beta\psi].$$

Hestenes [13] suggests taking $\lambda_{k+1} = \lambda_k - \beta\psi$. Then if $\psi(\mathbf{x}_{k+1}) = \mathbf{0}$ at the minimizer \mathbf{x}_{k+1} of $\mathcal{L}(\mathbf{x}, \lambda_{k+1})$

$$\mathbf{0} = \nabla_{\mathbf{x}}\mathcal{L} = \nabla_{\mathbf{x}}L = \nabla_{\mathbf{x}}\phi(\mathbf{x}_{k+1}) - \Gamma^T(\mathbf{x}_{k+1})\lambda_{k+1}$$

would yield $(\mathbf{x}_{k+1}, \lambda_{k+1}) = (\mathbf{x}^*, \lambda^*)$ satisfying the first-order necessary conditions (3).

The continuous-time version of Hestenes’ Method of Multipliers is $\dot{\lambda} = -\beta\psi$. This, coupled with steepest descent on \mathbf{x} , corresponds to choosing in (20):

$$\mathbf{P} = \begin{bmatrix} \mathbf{P}_{\mathbf{xx}} & \mathbf{P}_{\mathbf{x}\lambda} \\ \mathbf{P}_{\lambda\mathbf{x}} & \mathbf{P}_{\lambda\lambda} \end{bmatrix} = \begin{bmatrix} \mathbf{I}_n & \mathbf{0} \\ \mathbf{0} & -\beta\mathbf{I}_m \end{bmatrix}. \tag{22}$$

4.3 Newton’s method

For $\max_{\lambda} \min_{\mathbf{x}} \mathcal{L}(\mathbf{x}, \lambda)$ the first-order necessary conditions are

$$\mathbf{0} = \nabla_{\mathbf{x}}\mathcal{L} = \nabla_{\mathbf{x}}L + \beta\Gamma^T\psi, \quad \mathbf{0} = \nabla_{\lambda}\mathcal{L} = \nabla_{\lambda}L = -\psi. \tag{23}$$

Newton’s method applied to (23) is given by

$$\begin{bmatrix} \dot{\mathbf{x}} \\ \dot{\lambda} \end{bmatrix} = -\mathcal{H}^{-1}(\mathbf{y}) \begin{bmatrix} \nabla_{\mathbf{x}}\mathcal{L} \\ \nabla_{\lambda}\mathcal{L} \end{bmatrix} = -\mathcal{H}^{-1}(\mathbf{y}) \begin{bmatrix} \nabla_{\mathbf{x}}\mathcal{L} \\ -\psi \end{bmatrix}, \tag{24}$$

where

$$\mathcal{H}(\mathbf{y}) \triangleq \nabla_{\mathbf{y}}^2\mathcal{L} = \frac{\partial^2\mathcal{L}}{\partial\mathbf{y}^2} = \begin{bmatrix} \frac{\partial^2\mathcal{L}}{\partial\mathbf{x}^2} & -\Gamma^T \\ -\Gamma & \mathbf{0} \end{bmatrix}, \tag{25}$$

with $\Gamma(\mathbf{x})$ defined by (10). This corresponds to choosing in (20):

$$\mathbf{P} = \begin{bmatrix} \mathbf{P}_{\mathbf{xx}} & \mathbf{P}_{\mathbf{x}\lambda} \\ \mathbf{P}_{\lambda\mathbf{x}} & \mathbf{P}_{\lambda\lambda} \end{bmatrix} = \mathcal{H}^{-1}.$$

Instead of assuming \mathcal{H}^{-1} exists, Newton's method can be written as

$$\mathcal{H}(\mathbf{y}) \begin{bmatrix} \dot{\mathbf{x}} \\ \dot{\boldsymbol{\lambda}} \end{bmatrix} = \begin{bmatrix} \frac{\partial^2 \mathcal{L}}{\partial \mathbf{x}^2} & -\boldsymbol{\Gamma}^\top \\ -\boldsymbol{\Gamma} & \mathbf{0} \end{bmatrix} \begin{bmatrix} \dot{\mathbf{x}} \\ \dot{\boldsymbol{\lambda}} \end{bmatrix} = - \begin{bmatrix} \nabla_{\mathbf{x}} \mathcal{L} \\ \nabla_{\boldsymbol{\lambda}} \mathcal{L} \end{bmatrix}. \quad (26)$$

A geometric interpretation of Newton's method is given by noting that

$$\frac{d}{dt} \begin{bmatrix} \nabla_{\mathbf{x}} \mathcal{L} \\ \nabla_{\boldsymbol{\lambda}} \mathcal{L} \end{bmatrix} = \begin{bmatrix} \frac{\partial^2 \mathcal{L}}{\partial \mathbf{x}^2} \dot{\mathbf{x}} + \frac{\partial^2 \mathcal{L}}{\partial \boldsymbol{\lambda} \partial \mathbf{x}} \dot{\boldsymbol{\lambda}} \\ \frac{\partial^2 \mathcal{L}}{\partial \mathbf{x} \partial \boldsymbol{\lambda}} \dot{\mathbf{x}} + \frac{\partial^2 \mathcal{L}}{\partial \boldsymbol{\lambda}^2} \dot{\boldsymbol{\lambda}} \end{bmatrix} = \begin{bmatrix} \frac{\partial^2 \mathcal{L}}{\partial \mathbf{x}^2} & -\boldsymbol{\Gamma}^\top \\ -\boldsymbol{\Gamma} & \mathbf{0} \end{bmatrix} \begin{bmatrix} \dot{\mathbf{x}} \\ \dot{\boldsymbol{\lambda}} \end{bmatrix}. \quad (27)$$

Thus from (26)

$$\frac{d}{dt} \begin{bmatrix} \nabla_{\mathbf{x}} \mathcal{L} \\ \nabla_{\boldsymbol{\lambda}} \mathcal{L} \end{bmatrix} = - \begin{bmatrix} \nabla_{\mathbf{x}} \mathcal{L} \\ \nabla_{\boldsymbol{\lambda}} \mathcal{L} \end{bmatrix}. \quad (28)$$

Hence

$$\begin{bmatrix} \nabla_{\mathbf{x}} \mathcal{L} \\ \nabla_{\boldsymbol{\lambda}} \mathcal{L} \end{bmatrix}_t = e^{-t} \begin{bmatrix} \nabla_{\mathbf{x}} \mathcal{L} \\ \nabla_{\boldsymbol{\lambda}} \mathcal{L} \end{bmatrix}_{t=0} \quad \text{and we have} \quad \begin{bmatrix} \nabla_{\mathbf{x}} \mathcal{L} \\ \boldsymbol{\psi} \end{bmatrix}_t = e^{-t} \begin{bmatrix} \nabla_{\mathbf{x}} \mathcal{L} \\ \boldsymbol{\psi} \end{bmatrix}_{t=0} \rightarrow \begin{bmatrix} \mathbf{0} \\ \mathbf{0} \end{bmatrix} \quad \text{as } t \rightarrow \infty.$$

Thus Newton's method: a) is at least locally asymptotically stable to a point $\hat{\mathbf{y}}$ satisfying the necessary conditions (3) provided $\mathcal{H}^{-1}(\hat{\mathbf{y}})$ exists, b) is not stiff (all eigenvalues are $\mu = -1$), and c) has a domain of attraction that is the region containing $\hat{\mathbf{y}}$, where \mathcal{H}^{-1} exists. However, Newton's method may not be globally convergent. Furthermore, it only seeks stationary points of the augmented Lagrangian $\mathcal{L}(\mathbf{x}, \boldsymbol{\lambda})$, not specifically those yielding $\max_{\boldsymbol{\lambda}} \min_{\mathbf{x}} \mathcal{L}(\mathbf{x}, \boldsymbol{\lambda})$.

5 Stiff Differential Equations

Stiff systems are systems of differential equations which have two or more widely separated time scales, usually specified in terms of eigenvalues. For nonlinear systems we will use Lyapunov exponents.

5.1 Lyapunov exponents

Lyapunov exponents [14, p. 205] are generalizations of eigenvalues and characteristic (Floquet) multipliers that provide information about the (average) rates at which neighboring trajectories converge or diverge in a nonlinear system. Let $\mathbf{y}(t)$ and $\tilde{\mathbf{y}}(t)$ be solutions to

$$\dot{\mathbf{y}} = \mathbf{f}(\mathbf{y}), \quad (29)$$

starting from neighboring initial conditions, and let $\rho(t) = \|\tilde{\mathbf{y}}(t) - \mathbf{y}(t)\|$ be the distance between the trajectory $\mathbf{y}(t)$ and the perturbed trajectory $\tilde{\mathbf{y}}(t)$ at time t . If $\rho(0)$ is arbitrarily small and $\rho(t) \rightarrow \rho(0)e^{\sigma t}$ as $t \rightarrow \infty$ then σ is called a Lyapunov exponent for the reference trajectory $\mathbf{y}(t)$. The distance between the trajectory points $\mathbf{y}(t)$ and $\tilde{\mathbf{y}}(t)$ grows, shrinks, or remains constant for $\sigma > 0$, $\sigma < 0$, or $\sigma = 0$, respectively. In a p -dimensional state space there are p real Lyapunov exponents, $\sigma_1 \geq \dots \geq \sigma_p$, corresponding to exponential growth rates in p orthogonal directions. For a given trajectory

$\mathbf{y}(t)$ the Lyapunov exponents are unique, but are functions of the initial state. Arbitrarily close initial states (*e.g.*, on and to either side of a separatrix) may yield trajectories with different Lyapunov exponents, corresponding to different behaviors as $t \rightarrow \infty$.

If $\mathbf{f}(\cdot)$ is continuous and continuously differentiable the Lyapunov exponents can be calculated in terms of the state perturbation equations

$$\dot{\boldsymbol{\eta}} = \mathbf{A}(t)\boldsymbol{\eta}, \quad \mathbf{A}(t) = \frac{\partial \mathbf{f}[\mathbf{y}(t)]}{\partial \mathbf{y}}, \tag{30}$$

where $\mathbf{A}(t)$ is evaluated along a trajectory $\mathbf{y}(t)$ and, for small α , $\tilde{\mathbf{y}}(t) = \mathbf{y}(t) + \alpha\boldsymbol{\eta}(t) + \mathbf{O}(\alpha^2)$ is an initially neighboring trajectory. If $\mathbf{f}(\cdot)$ is discontinuous across some “switching surface” in state space certain “jump conditions” must be imposed to accurately compute Lyapunov exponents [15].

For the special case of an equilibrium $\mathbf{y}(t) = \text{constant}$, so that \mathbf{A} is constant, the Lyapunov exponents σ_k are the real parts of the eigenvalues μ_k , $k = 1, \dots, p$, of \mathbf{A} . The same result holds for trajectories that asymptotically approach an equilibrium.

One way to compute Lyapunov exponents numerically [16] is to integrate the equations of motion (29), along with p copies of the perturbation equations (30), one for each of p initially orthogonal unit perturbations $\boldsymbol{\eta}_k(0)$, corresponding to the semi-axes of an initially spherical p -dimensional ellipsoid in state space. At $t > 0$ we define the instantaneous Lyapunov exponents as

$$\sigma_k(t) = \frac{1}{t} \ln \left[\frac{\|\boldsymbol{\eta}_k(t)\|}{\|\boldsymbol{\eta}_k(0)\|} \right] \tag{31}$$

with the Lyapunov exponents $\sigma_k = \lim_{t \rightarrow \infty} \{\sigma_k(t)\}$. We define the instantaneous “stiffness” as $\Sigma(t) \triangleq |\sigma_{\max}(t) - \sigma_{\min}(t)|$. As the trajectory $\mathbf{y}(t)$ moves through state space, the perturbation vectors $\boldsymbol{\eta}_k(t)$ rotate (so they are no longer orthogonal) and stretch or shrink as the axes of the ellipsoid centered at $\mathbf{y}(t)$ change. Over time, the perturbation vectors will all tend to align with the major axis of the ellipse, corresponding to the largest Lyapunov exponent, in a manner analogous to the power method for generating the dominant eigenvalue and eigenvector of a matrix. Since some of the Lyapunov exponents may be positive, particularly in chaotic systems, the algorithm incorporates a periodic discontinuous rescaling of the perturbation vectors, to avoid numerical overflow, using a Gram-Schmidt orthonormalization procedure [14, p. 207].

5.2 State perturbation equations

Let $\mathbf{p}_k^T(\mathbf{y})$, $k = 1, \dots, p$, denote the k -th row of $\mathbf{P}(\mathbf{y})$. Then

$$\dot{\mathbf{y}} = \mathbf{f}(\mathbf{y}) = -\mathbf{P}(\mathbf{y})\nabla_{\mathbf{y}}\mathcal{L}(\mathbf{y}) = - \begin{bmatrix} \mathbf{p}_1^T(\mathbf{y}) \\ \vdots \\ \mathbf{p}_p^T(\mathbf{y}) \end{bmatrix} \nabla_{\mathbf{y}}\mathcal{L}(\mathbf{y}).$$

Along a trajectory $\mathbf{y}(t)$ the state perturbation equations (30), with $\mathbf{A}(\mathbf{y}) = \partial \mathbf{f}(\mathbf{y})/\partial \mathbf{y}$, are given by

$$\mathbf{A}(\mathbf{y}) = -\mathbf{P}(\mathbf{y})\mathcal{H}(\mathbf{y}) - \begin{bmatrix} \frac{\partial \mathcal{L}(\mathbf{y})}{\partial \mathbf{y}} \frac{\partial \mathbf{p}_1(\mathbf{y})}{\partial \mathbf{y}} \\ \vdots \\ \frac{\partial \mathcal{L}(\mathbf{y})}{\partial \mathbf{y}} \frac{\partial \mathbf{p}_p(\mathbf{y})}{\partial \mathbf{y}} \end{bmatrix}, \tag{32}$$

where $\mathcal{H} = \nabla_{\mathbf{y}}^2 \mathcal{L}(\mathbf{y}) = \partial^2 \mathcal{L} / \partial \mathbf{y}^2$. At a stationary point \mathbf{y}^* of $\mathcal{L}(\mathbf{y})$, $\nabla_{\mathbf{y}} \mathcal{L}(\mathbf{y}^*) = \mathbf{0}$ and $\mathbf{A}(\mathbf{y}^*) = -\mathbf{P}(\mathbf{y}^*) \mathcal{H}(\mathbf{y}^*)$. This result also holds for \mathbf{P} constant. The eigenvalues of $\mathbf{A}(\mathbf{y}^*)$ provide a measure of the stiffness of the system (29), at least near \mathbf{y}^* . Along a trajectory $\mathbf{y}(t)$ the Lyapunov exponents (31) do so.

6 Unconstrained Min-Max Saddle Point

In [8] a Gradient Enhanced Min-Max (GEMM) algorithm is developed as a variable Levenberg-Marquardt modification [17, p. 145] to Newton's method, designed to find saddle points of a scalar-valued function. The GEMM algorithm specifically seeks min-max saddle points, whereas Newton's method seeks stationary points. As we shall see, GEMM generally has a larger domain of attraction than Newton's method (by keeping the Hessian matrix nonsingular), is not stiff, and is faster than Newton's method.

As background we summarize some results from [8] for GEMM applied to the problem of finding a game-theoretic saddle point in the absence of equality constraints.

Let \mathbf{M}^T denote the transpose of a matrix \mathbf{M} . For $\mathbf{y}^T = [\mathbf{u}^T, \mathbf{v}^T]$, with $\mathbf{u} \in \mathcal{U} \subseteq R^n$, $\mathbf{v} \in \mathcal{V} \subseteq R^m$, and $\mathbf{y} \in R^p$, $p = n + m$, we are concerned with finding a point $\mathbf{y}^* = (\mathbf{u}^*, \mathbf{v}^*)$ to yield a min-max for a C^2 scalar-valued function $\phi(\mathbf{y}) = \phi(\mathbf{u}, \mathbf{v})$, such that \mathbf{u}^* minimizes ϕ and \mathbf{v}^* maximizes ϕ . That is, $\phi(\mathbf{u}^*, \mathbf{v}) \leq \phi(\mathbf{u}^*, \mathbf{v}^*) \leq \phi(\mathbf{u}, \mathbf{v}^*)$ for all $\mathbf{u} \in \mathcal{U}$ and $\mathbf{v} \in \mathcal{V}$. Denote the gradient of ϕ by

$$\mathbf{g} = \left[\frac{\partial \phi}{\partial \mathbf{y}} \right]^T = \begin{bmatrix} \mathbf{g}_u \\ \mathbf{g}_v \end{bmatrix} = \begin{bmatrix} \left[\frac{\partial \phi}{\partial \mathbf{u}} \right]^T \\ \left[\frac{\partial \phi}{\partial \mathbf{v}} \right]^T \end{bmatrix}$$

and the Hessian of ϕ by

$$\mathbf{G} = \frac{\partial^2 \phi}{\partial \mathbf{y}^2} = \begin{bmatrix} \mathbf{G}_{uu} & \mathbf{G}_{uv} \\ \mathbf{G}_{uv}^T & \mathbf{G}_{vv} \end{bmatrix},$$

where $\mathbf{g}_u \in R^n$, $\mathbf{g}_v \in R^m$, $\mathbf{G}_{uu} = \partial^2 \phi / \partial \mathbf{u}^2 \in R^{n \times n}$, $\mathbf{G}_{vv} = \partial^2 \phi / \partial \mathbf{v}^2 \in R^{m \times m}$, and $\mathbf{G}_{uv} = \partial^2 \phi / \partial \mathbf{u} \partial \mathbf{v} \in R^{n \times m}$.

We are particularly concerned with finding a **proper stationary min-max point** \mathbf{y}^* , at which:

1. $\phi(\mathbf{u}^*, \mathbf{v}) < \phi(\mathbf{u}^*, \mathbf{v}^*) < \phi(\mathbf{u}, \mathbf{v}^*)$ for all $\mathbf{u} \in \mathcal{U} - \{\mathbf{u}^*\}$ and $\mathbf{v} \in \mathcal{V} - \{\mathbf{v}^*\}$,
2. $\mathbf{g}^* = \mathbf{g}(\mathbf{y}^*) = \mathbf{0}$,
3. $\mathbf{G}_{uu}^* = \mathbf{G}_{uu}(\mathbf{y}^*) \geq 0$ (positive semidefinite),
4. $\mathbf{G}_{vv}^* = \mathbf{G}_{vv}(\mathbf{y}^*) \leq 0$ (negative semidefinite),
5. $|\mathbf{G}^*| = |\mathbf{G}(\mathbf{y}^*)| < 0$,

where $|\cdot|$ denotes the determinant. In addition we assume that $\mathbf{g}(\mathbf{y}) \neq \mathbf{0}$ for $\mathbf{y} \neq \mathbf{y}^*$ and that $\|\mathbf{g}(\mathbf{y})\| \rightarrow \infty$ as $\|\mathbf{y} - \mathbf{y}^*\| \rightarrow \infty$, where $\|\cdot\|$ denotes the Euclidian norm.

For $\mathbf{u} \in \mathcal{U}$ and $\mathbf{v} \in \mathcal{V}$ let

$$\mathcal{R}_u = \{(\mathbf{u}, \mathbf{v}) : \mathbf{v} \in \mathcal{V} \text{ and } \phi(\mathbf{u}, \mathbf{v}) \leq \phi(\bar{\mathbf{u}}, \mathbf{v}) \text{ for all } \bar{\mathbf{u}} \in \mathcal{U}, \}$$

denote the rational reaction set for the minimizing player \mathbf{u} , and let

$$\mathcal{R}_v = \{(\mathbf{u}, \mathbf{v}) : \mathbf{u} \in \mathcal{U} \text{ and } \phi(\mathbf{u}, \bar{\mathbf{v}}) \leq \phi(\mathbf{u}, \mathbf{v}) \text{ for all } \bar{\mathbf{v}} \in \mathcal{V}\}$$

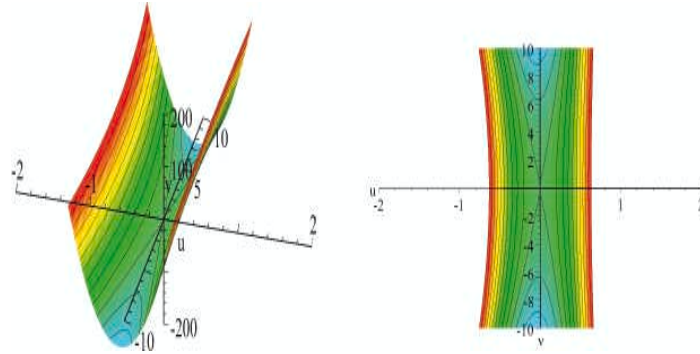


Figure 1: Banana saddle ($a = 1000, c = 1$).

denote the rational reaction set for the maximizing player \mathbf{v} . On \mathcal{R}_u with $\mathbf{u} \in \overset{\circ}{\mathcal{U}}$ (interior of \mathcal{U}) it is necessary [9, p. 149] that

$$\mathbf{0} = \mathbf{g}_u(\mathbf{u}, \mathbf{v}) = \left[\frac{\partial \phi(\mathbf{u}, \mathbf{v})}{\partial \mathbf{u}} \right]^\top \tag{33}$$

and

$$\mathbf{G}_{uu}(\mathbf{u}, \mathbf{v}) = \frac{\partial^2 \phi(\mathbf{u}, \mathbf{v})}{\partial \mathbf{u}^2} \geq 0.$$

On \mathcal{R}_v with $\mathbf{v} \in \overset{\circ}{\mathcal{V}}$ it is necessary that

$$\mathbf{0} = \mathbf{g}_v(\mathbf{u}, \mathbf{v}) = \left[\frac{\partial \phi(\mathbf{u}, \mathbf{v})}{\partial \mathbf{v}} \right]^\top \tag{34}$$

and

$$\mathbf{G}_{vv}(\mathbf{u}, \mathbf{v}) = \frac{\partial^2 \phi(\mathbf{u}, \mathbf{v})}{\partial \mathbf{v}^2} \leq 0.$$

6.1 Stingray saddle function

For $a > 0$ and $c > 0$ we consider the “Stingray” saddle function

$$\phi = \frac{a}{2}u^2 + \frac{c}{2}(u - 1)v^2 \tag{35}$$

with gradient and Hessian

$$\mathbf{g} = \begin{bmatrix} g_u \\ g_v \end{bmatrix} = \begin{bmatrix} au + \frac{c}{2}v^2 \\ c(u - 1)v \end{bmatrix}, \quad \mathbf{G} = \begin{bmatrix} G_{uu} & G_{uv} \\ G_{uv} & G_{vv} \end{bmatrix} = \begin{bmatrix} a & cv \\ cv & c(u - 1) \end{bmatrix}.$$

The function has a unique proper min-max point at $\mathbf{y}^* = (u^*, v^*) = (0, 0)$, with $\mathbf{g} \neq \mathbf{0}$ for $\mathbf{y} \neq \mathbf{0}$ and $\|\mathbf{g}\| \rightarrow \infty$ as $\|\mathbf{y}\| \rightarrow \infty$. Note that $|\mathbf{G}| = ac(u - 1) - c^2v^2 = 0$ on $u = 1 + \frac{c}{a}v^2$. Also note that $G_{uu} = a > 0$ for all (u, v) , but $G_{vv} = c(u - 1) < 0$ only for $u < 1$. The Stingray function $\phi(u, v)$ is convex in u for each v , but is concave in v only for $u < 1$. For $u > 1$ the function is convex in v .

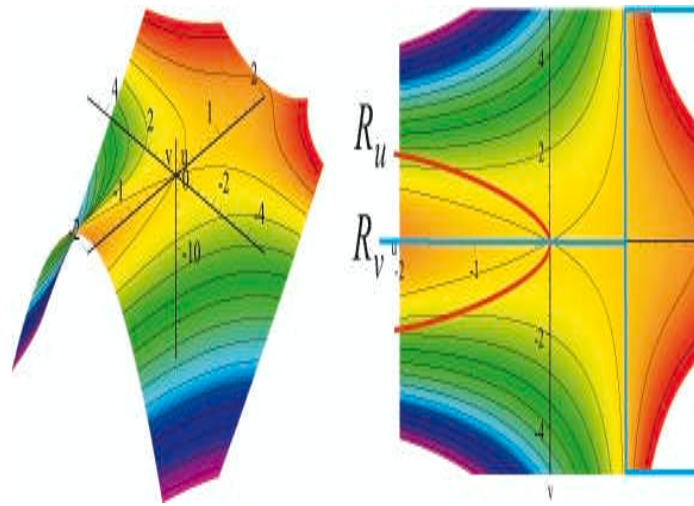


Figure 2: Stingray saddle ($a = 1, c = 1$).

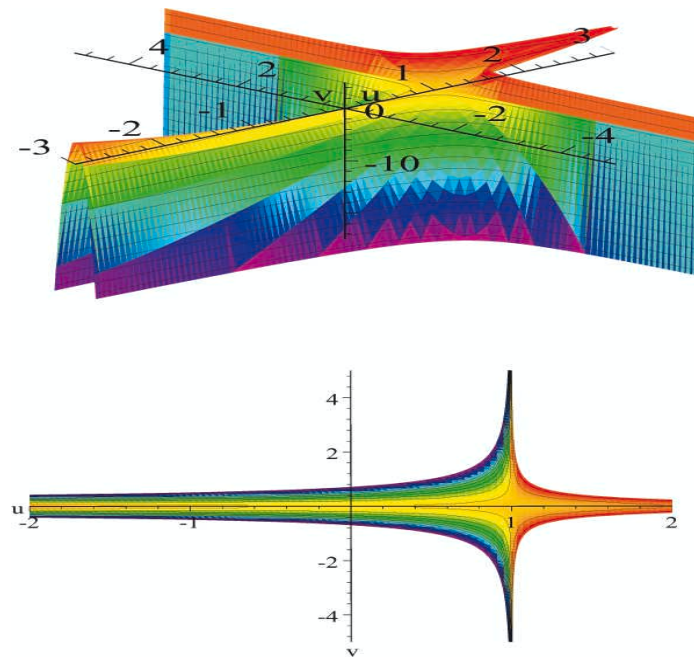


Figure 3: Stingray saddle ($a = 1, c = 100$).

Figures 1–3 show three-dimensional and contour plots for various values of a and c . For $a = 1000$ and $c = 1$ the function is similar to Rosenbrock’s “banana” function, having a steep-walled canyon with a parabolic valley, except that the stationary point is a saddle point instead of a minimum point. For $a = 1$ and increasing values of c the function looks like a stingray flapping its wings. Unless otherwise specified, we will consider the case where $a = 1$ and $c = 100$. For these parameter values the stingray function has a sharp local \max_v ridge on $v = 0, u < 1$, and a local \max_u valley on $u = -\frac{c}{2a}v^2$.

As illustrated in Figure 2, the $\min_u \max_v \phi$ rational reaction sets, for $v_{\min} \leq v \leq v_{\max}$ with $v_{\max} > 0$ and $v_{\min} < 0$, are

$$\mathcal{R}_u = \left\{ (u, v) : u = -\frac{c}{2a}v^2 \right\}, \quad \mathcal{R}_v = \{ (u, v) : v = v^\circ(u) \},$$

where

$$v^\circ(u) = \begin{cases} 0 & \text{if } u < 1, \\ \in [v_{\min}, v_{\max}] & \text{if } u = 1, \\ v_{\max} & \text{if } u > 1 \text{ and } v_{\max} \geq |v_{\min}|, \\ v_{\min} & \text{if } u > 1 \text{ and } v_{\max} \leq |v_{\min}|. \end{cases}$$

In particular, while the minimizing player u seeks $g_u = 0$, the maximizing player v only seeks $g_v = 0$ for $u < 1$. For $u > 1$ the maximizing player seeks either the upper or lower bound on v . Nevertheless, the intersection $\mathcal{R}_u \cap \mathcal{R}_v$ of the reaction sets is the min-max point $u^* = v^* = 0$, where both $g_u = 0$ and $g_v = 0$.

6.2 Gradient enhanced Newton (GEN) minimization

Consider, for a moment, Newton’s method applied to the problem of finding a unique proper *minimum* point for a function $\phi(\mathbf{y})$. For the case where $\mathbf{G}(\mathbf{y}) = \partial^2\phi/\partial\mathbf{y}^2$ is not positive definite everywhere, the Levenberg–Marquardt modification to Newton’s method [17, pp. 145–149] is given by $(\alpha\mathbf{I} + \mathbf{G})\dot{\mathbf{y}} = -\mathbf{g}$, where $\alpha \geq 0$ and \mathbf{I} denotes the $p \times p$ identity matrix. If $\mathbf{F} = \alpha\mathbf{I} + \mathbf{G}$ is positive definite, then let $\dot{\mathbf{y}} = -\mathbf{P}(\mathbf{y})\mathbf{g}$, with $\mathbf{P}(\mathbf{y}) = \mathbf{F}^{-1} = (\alpha\mathbf{I} + \mathbf{G})^{-1}$. Then $\dot{\phi} = \mathbf{g}^\top\dot{\mathbf{y}} = -\mathbf{g}^\top\mathbf{P}\mathbf{g} < 0$ for $\mathbf{g} \neq \mathbf{0}$ establishes (global) asymptotic stability.

Let μ_i and $\boldsymbol{\xi}_i, i = 1, \dots, p$, denote the eigenvalues and eigenvectors of \mathbf{G} , respectively. For symmetric \mathbf{G} the eigenvalues are all real, but may not all be positive. The matrix $\mathbf{F} = \alpha\mathbf{I} + \mathbf{G}$ has eigenvalues $\omega_i = \mu_i + \alpha$ and eigenvectors $\boldsymbol{\xi}_i$, since $\mathbf{F}\boldsymbol{\xi}_i = (\mu_i + \alpha)\boldsymbol{\xi}_i$. Thus, at a point \mathbf{y} , if α is sufficiently large all of the eigenvalues of \mathbf{F} will be positive. As $\alpha \rightarrow 0$ the method approaches Newton’s method applied to $\phi(\mathbf{y})$, and as $\alpha \rightarrow \infty$ the method approaches Steepest Descent applied to $\phi(\mathbf{y})/\alpha$.

The Levenberg–Marquardt minimization method generally will not work with constant α . If $|\mathbf{G}(\mathbf{y})|$ changes sign somewhere then for constant α the determinant $|\mathbf{F}| = |\alpha\mathbf{I} + \mathbf{G}|$ will also generally change sign, although at a different place than $|\mathbf{G}(\mathbf{y})|$.

In [7] we develop a **Gradient Enhanced Newton** (GEN) minimization method, in which $\alpha = \gamma \|\mathbf{g}\| = \gamma\sqrt{\mathbf{g}^\top\mathbf{g}}$ with constant $\gamma \geq 0$, yielding

$$\dot{\mathbf{y}} = -\mathbf{P}(\mathbf{y})\mathbf{g} = -[\gamma \|\mathbf{g}\| \mathbf{I} + \mathbf{G}]^{-1} \mathbf{g}. \tag{36}$$

The ideas behind this minimization method are: 1) at points where $\|\mathbf{g}\| \neq 0$ we can make \mathbf{F} be positive definite for sufficiently large $\gamma \geq 0$; 2) for small γ or near places where $\mathbf{g} = \mathbf{0}$ the method behaves like Newton’s method; 3) the speed $\|\dot{\mathbf{y}}\| \approx 1/\gamma$. In [7] it is shown that, for sufficiently large $\gamma \geq 0$, GEN is globally asymptotically stable for functions that

have a single proper stationary minimum point and satisfy a Lyapunov growth condition. In addition, when applied to Rosenbrock's "banana" function, GEN is uniformly nonstiff and approximately 25 times faster than Newton's method and approximately 2500 times faster than Steepest Descent.

A very recent paper [18] shows that, for long-term optimization algorithms, Levenberg–Marquardt, especially in the form (36), is more fundamental than Newton's method and that Newton's method should be viewed as a special case of Levenberg–Marquardt, rather than the other way around.

6.3 Gradient enhanced min-max

The Levenberg–Marquardt modification of Newton's method can not be used for min-max problems, but a variation of it can. Consider the Hessian

$$\mathbf{G}(\mathbf{y}) = \frac{\partial^2 \phi}{\partial \mathbf{y}^2} = \begin{bmatrix} \frac{\partial^2 \phi}{\partial u^2} & \frac{\partial^2 \phi}{\partial u \partial v} \\ \frac{\partial^2 \phi}{\partial v \partial u} & \frac{\partial^2 \phi}{\partial v^2} \end{bmatrix} = \begin{bmatrix} \mathbf{G}_{uu} & \mathbf{G}_{uv} \\ \mathbf{G}_{uv}^\top & \mathbf{G}_{vv} \end{bmatrix},$$

which is positive definite at a proper minimum point. But at a proper min-max point \mathbf{y}^* we have $\mathbf{G}_{uu}^* = \mathbf{G}_{uu}(\mathbf{y}^*) \geq 0$, $\mathbf{G}_{vv}^* = \mathbf{G}_{vv}(\mathbf{y}^*) \leq 0$, and $|\mathbf{G}^*| = |\mathbf{G}(\mathbf{y}^*)| < 0$. Thus the eigenvalues of \mathbf{G}_{uu}^* are ≥ 0 , the eigenvalues of \mathbf{G}_{vv}^* are ≤ 0 , and the product of the eigenvalues of \mathbf{G}^* is negative. When $|\mathbf{G}(\mathbf{y})|$ passes through zero, so does one or more of its eigenvalues. The Levenberg-Marquardt matrix $\mathbf{F} = \alpha \mathbf{I} + \mathbf{G}$ could be used to make *all* of its eigenvalues be positive (or *all* of them negative, for $\alpha < 0$) at any given point $\hat{\mathbf{y}}$. But if $\alpha = \alpha(\mathbf{y}) \geq 0$, with $\alpha(\mathbf{y}^*) = 0$ and $|\mathbf{G}^*| = |\mathbf{G}(\mathbf{y}^*)| < 0$, then somewhere between \mathbf{y}^* and $\hat{\mathbf{y}}$ we would have $|\mathbf{F}(\mathbf{y})| = 0$, as one of the positive eigenvalues goes negative or one of the negative eigenvalues goes positive. What we need to do, to ensure that the replacement matrix $\mathbf{F}(\mathbf{y})$ for $\mathbf{G}(\mathbf{y})$ is nonsingular, is to keep the positive eigenvalues positive and the negative eigenvalues negative, yielding $|\mathbf{F}(\mathbf{y})| < 0$.

Consider

$$\dot{\mathbf{y}} = -\mathbf{P}\mathbf{g} \tag{37}$$

with

$$\mathbf{P} = \mathbf{F}^{-1} = \begin{bmatrix} \alpha_u \mathbf{I}_u + \mathbf{G}_{uu} & \mathbf{G}_{uv} \\ \mathbf{G}_{uv}^\top & -\alpha_v \mathbf{I}_v + \mathbf{G}_{vv} \end{bmatrix}^{-1}. \tag{38}$$

For $\alpha_u = \alpha_v = \alpha \rightarrow \infty$ the method approaches Min-Max Ascent (see Section 6.4.1) applied to ϕ/α . For $\alpha \rightarrow 0$ the method approaches Newton's method applied to ϕ . The **Gradient Enhanced Min-Max** (GEMM) method is given by (37)–(38) with $\alpha_u = \gamma_u \|\mathbf{g}\|$ and $\alpha_v = \gamma_v \|\mathbf{g}\|$ for constants $\gamma_u \geq 0$ and $\gamma_v \geq 0$. That is, $\mathbf{P} = \mathbf{F}^{-1}$, with

$$\mathbf{F} = \begin{bmatrix} \gamma_u \|\mathbf{g}\| \mathbf{I}_u + \mathbf{G}_{uu} & \mathbf{G}_{uv} \\ \mathbf{G}_{uv}^\top & -\gamma_v \|\mathbf{g}\| \mathbf{I}_v + \mathbf{G}_{vv} \end{bmatrix}. \tag{39}$$

In [8] we prove that for sufficiently large constants $\gamma_u \geq 0$ and $\gamma_v \geq 0$ the matrix \mathbf{F} in (39) is nonsingular for all \mathbf{y} . Hence the only equilibrium for (37)–(39) is at \mathbf{y}^* . A Lyapunov approach can be used to investigate whether the unique equilibrium at \mathbf{y}^* is (globally) asymptotically stable. However, note that using $W(\mathbf{y}) = \mathbf{g}^\top \mathbf{g}$ as a descent function [14, p. 276] would not work, since $\dot{W} = \mathbf{g}^\top \dot{\mathbf{g}} + \dot{\mathbf{g}}^\top \mathbf{g} = \mathbf{g}^\top \mathbf{G} \dot{\mathbf{y}} + \dot{\mathbf{y}}^\top \mathbf{G} \mathbf{g} = -\mathbf{g}^\top \mathbf{Q} \mathbf{g}$, with $\mathbf{Q} = \mathbf{G}\mathbf{P} + \mathbf{P}^\top \mathbf{G}$ not being positive definite if $|\mathbf{G}|$ changes sign (see Lyapunov's lemma [14, p. 223]). Also note that replacing the $\min_u \max_v \phi$ problem with Newton's

method (or the Levenberg–Marquardt modification) applied to the least squares problem [17, pp. 146–148] of minimizing $W(\mathbf{y})$, via $\dot{\mathbf{y}} = -\mathbf{H}^{-1}(\mathbf{y})\nabla W$, where $\nabla W = [\partial W/\partial \mathbf{y}]^\top$ and $\mathbf{H}(\mathbf{y}) = \partial^2 W/\partial \mathbf{y}^2$, would involve third derivatives of $\phi(\mathbf{y})$.

6.4 Gradient transformation results for the stingray saddle function

6.4.1 Min-max ascent

Since \mathbf{u} seeks $\min_u \phi(\mathbf{u}, \mathbf{v})$ and \mathbf{v} seeks $\max_v \phi(\mathbf{u}, \mathbf{v})$, the first min-max algorithm investigated by researchers [3] was steepest descent on \mathbf{u} and steepest ascent on \mathbf{v} .

Let \mathbf{I}_u and \mathbf{I}_v denote the $n \times n$ and $m \times m$ identity matrices, respectively. Taking

$$\mathbf{P}(\mathbf{y}) = \text{diag} [\mathbf{I}_u, -\mathbf{I}_v] = \begin{bmatrix} \mathbf{I}_u & \mathbf{0} \\ \mathbf{0} & -\mathbf{I}_v \end{bmatrix}$$

yields the **Min-Max Ascent** algorithm

$$\dot{\mathbf{u}} = -\mathbf{g}_u, \quad \dot{\mathbf{v}} = \mathbf{g}_v \tag{40}$$

with the state perturbation equations

$$\begin{bmatrix} \dot{\boldsymbol{\eta}}_u \\ \dot{\boldsymbol{\eta}}_v \end{bmatrix} = \begin{bmatrix} -\mathbf{G}_{uu} & -\mathbf{G}_{uv} \\ \mathbf{G}_{uv}^\top & \mathbf{G}_{vv} \end{bmatrix} \begin{bmatrix} \boldsymbol{\eta}_u \\ \boldsymbol{\eta}_v \end{bmatrix}.$$

For the Stingray saddle function

$$\phi = \frac{a}{2}u^2 + \frac{c}{2}(u-1)v^2$$

the Min-Max Ascent system is given by

$$\dot{u} = -g_u = -au - \frac{c}{2}v^2, \quad \dot{v} = g_v = c(u-1)v$$

with the state perturbation equations

$$\begin{bmatrix} \dot{\boldsymbol{\eta}}_u \\ \dot{\boldsymbol{\eta}}_v \end{bmatrix} = \begin{bmatrix} -a & -cv \\ cv & c(u-1) \end{bmatrix} \begin{bmatrix} \boldsymbol{\eta}_u \\ \boldsymbol{\eta}_v \end{bmatrix}.$$

At the stationary point the state perturbation matrix

$$\mathbf{A}(\mathbf{y}^*) = \begin{bmatrix} -a & 0 \\ 0 & -c \end{bmatrix}$$

has eigenvalues $\{-a, -c\}$. For $a = 1$ and $c = 100$ Min-Max Ascent yields a very stiff system.

Figure 4 shows Min-Max Ascent trajectories for the case where $a = 1$ and $c = 100$. For numerical integration we use fixed step size ($\Delta t = 10^{-5}$, because of stiffness) standard 4th-order Runge-Kutta. Trajectories for $u < 1$ rapidly approach the $v = 0$ ($g_v = 0$) surface (the sharp local maximum ridge of the Stingray) and then slowly move along the ridge toward the saddle point at the origin. This is caused by the stiffness of the system. Notice the tendency, in the region $u > 1$, for trajectories to diverge from the $g_v = 0$ surface rather than converge to it. This is caused by G_{vv} not being negative definite everywhere.

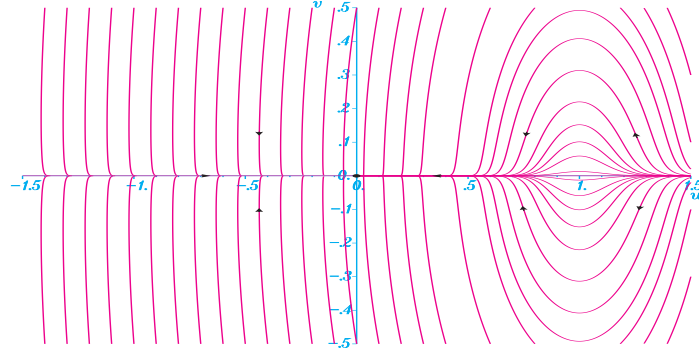


Figure 4: Min-Max Ascent ($a = 1$, $c = 100$).

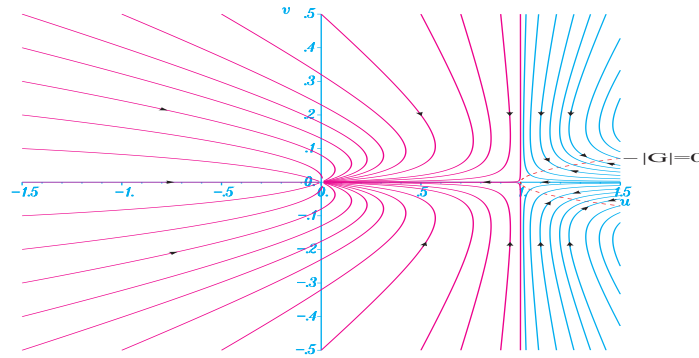


Figure 5: Newton's method ($a = 1$, $c = 100$).

6.4.2 Newton's method

Newton's method, in which $d\mathbf{g}/dt = -\mathbf{g}$, [hence, $\mathbf{g}(t) = \mathbf{g}(0)e^{-t} \rightarrow \mathbf{0}$ as $t \rightarrow \infty$], corresponds to $\mathbf{P}(\mathbf{y}) = \mathbf{G}^{-1}(\mathbf{y})$. Applied to the Stingray saddle function, Newton's method is given by

$$\begin{aligned} \dot{\mathbf{y}} &= -\mathbf{G}^{-1}\mathbf{g} \\ &= -\begin{bmatrix} a & cv \\ cv & c(u-1) \end{bmatrix}^{-1} \begin{bmatrix} au + \frac{c}{2}v^2 \\ c(u-1)v \end{bmatrix} = -\frac{c}{|\mathbf{G}|} \begin{bmatrix} (u-1)(au + \frac{1}{2}cv^2) - cv^2(u-1) \\ -v(au + \frac{1}{2}cv^2) + a(u-1)v \end{bmatrix}, \end{aligned} \quad (41)$$

where $|\mathbf{G}| = ac(u-1) - c^2v^2$. Figure 5 shows trajectories for Newton's method applied to the Stingray saddle function ($a = 1$, $c = 100$) using 4th-order Runge-Kutta ($\Delta t = 10^{-3}$).

At $\mathbf{y}^* = (u^*, v^*) = (0, 0)$ the state perturbation equations yield

$$\mathbf{A}(\mathbf{y}^*) = \begin{bmatrix} -1 & 0 \\ 0 & -1 \end{bmatrix}$$

with eigenvalues $\{-1, -1\}$. This is clearly not a stiff system near \mathbf{y}^* . Trajectories move at a much better speed than in Min-Max Ascent, as indicated by the step size. However,

Newton’s method is not globally asymptotically stable to \mathbf{y}^* . Note that solutions to (41) only exist for $|\mathbf{G}| \neq 0$ and that $|\mathbf{G}| = 0$ on $v^2 = (u - 1)a/c$. The domain of attraction to \mathbf{y}^* is only the region $u < 1$, that is, the region where $\mathbf{G}_{vv} < 0$.

6.4.3 GEMM

For a and $c > 0$ in the Stingray saddle function (35) consider

$$\mathbf{F} = \begin{bmatrix} \alpha_u \mathbf{I}_u + \mathbf{G}_{uu} & \mathbf{G}_{uv} \\ \mathbf{G}_{uv}^\top & -\alpha_v \mathbf{I}_v + \mathbf{G}_{vv} \end{bmatrix} = \begin{bmatrix} \alpha_u + a & cv \\ cv & -\alpha_v + c(u - 1) \end{bmatrix}.$$

The determinant $|\mathbf{F}| = (\alpha_u + a)[-\alpha_v + c(u - 1)] - c^2v^2$ is zero on $c^2v^2 = (\alpha_u + a)[-\alpha_v + c(u - 1)]$ provided $-\alpha_v + c(u - 1) \geq 0$. Since $\alpha_u + a > 0$ for all $\alpha_u \geq 0$ with $a > 0$ and $c > 0$, a necessary and sufficient condition for $|\mathbf{F}(u, v)| < 0$ for all u, v is that $-\alpha_v \mathbf{I}_v + \mathbf{G}_{vv} = -\alpha_v + c(u - 1) < 0$ for all u . We can ensure that $|\mathbf{F}(u, v)| < 0$ for all u, v by taking

$$\alpha_v = \gamma_v \|\mathbf{g}\| = \gamma_v \sqrt{\left(au + \frac{c}{2}v^2\right)^2 + c^2(u - 1)^2v^2}$$

with sufficiently large $\gamma_v > 0$. Then

$$|\mathbf{F}| = -\gamma_v(\alpha_u + a) \sqrt{\left(au + \frac{c}{2}v^2\right)^2 + c^2(u - 1)^2v^2} + (\alpha_u + a)c(u - 1) - c^2v^2.$$

The $\max_v |\mathbf{F}|$ occurs on $v = 0$, with

$$|\mathbf{F}|_{v=0} = -\gamma_v(\alpha_u + a) \sqrt{(au)^2} + (\alpha_u + a)c(u - 1) = (\alpha_u + a)[-\gamma_v a|u| + c(u - 1)].$$

For $u \leq 0$ we have $|\mathbf{F}|_{v=0} < 0$. For $u > 0$ we have

$$0 = |\mathbf{F}|_{v=0} = (\alpha_u + a)[-\gamma_v au + c(u - 1)] = (\alpha_u + a)[(c - \gamma_v a)u - c]$$

at

$$u = \frac{1}{1 - \gamma_v \frac{a}{c}}$$

which yields $u < 0$ (a contradiction) for $\gamma_v > c/a$. We conclude that $|\mathbf{F}(u, v)| < 0$ for all u, v if we take $\alpha_u = \gamma_u \|\mathbf{g}\|$ and $\alpha_v = \gamma_v \|\mathbf{g}\|$, with $\gamma_u \geq 0$ and $\gamma_v > c/a$.

Applied to the Stingray function, the Gradient Enhanced Min-Max algorithm is given by

$$\begin{bmatrix} \dot{u} \\ \dot{v} \end{bmatrix} = -\mathbf{F}^{-1} \mathbf{g} = -\frac{1}{|\mathbf{F}|} \begin{bmatrix} [-\gamma_v \|\mathbf{g}\| + c(u - 1)](au + \frac{1}{2}cv^2) - c^2v^2(u - 1) \\ -cv(au + \frac{1}{2}cv^2) + (\gamma_u \|\mathbf{g}\| + a)c(u - 1)v \end{bmatrix},$$

where $0 > |\mathbf{F}| = (\gamma_u \|\mathbf{g}\| + a)[-\gamma_v \|\mathbf{g}\| + c(u - 1)] - c^2v^2$ for all u, v , provided $\gamma_u \geq 0$ and $\gamma_v > c/a$. For $a = 1$, $c = 100$, and $\gamma_v = 101$, Figures 6–7 show trajectories for the Gradient Enhanced Min-Max algorithm for $\gamma_u = 1$ and 10, respectively.

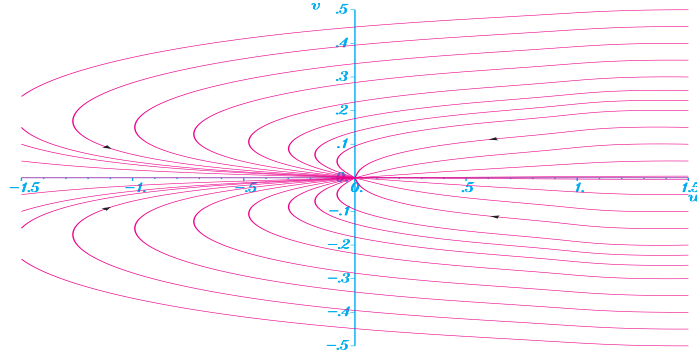


Figure 6: GEMM trajectories ($\gamma_u = 1$, $\gamma_v = 101$).

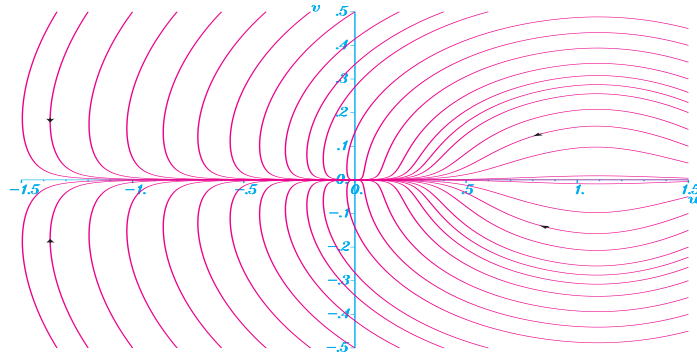


Figure 7: GEMM trajectories ($\gamma_u = 10$, $\gamma_v = 101$).

6.4.4 Unconstrained trajectory following performance comparisons

For comparison of Min-Max Ascent, Newton’s method, and the Gradient Enhanced Min-Max (GEMM) method, we consider the trajectories starting from $(u, v) = (-1.5, 0.5)$ for the Stingray saddle function. We use fixed time step standard 4th-order Runge-Kutta with the time step Δt chosen to control the approximate initial displacement $\Delta s = \|\dot{\mathbf{y}}(0)\| \Delta t$. The trajectories are terminated when $\|\mathbf{g}\| < 10^{-3}$. We consider two cases: Table 1 shows results for the “Banana saddle” ($a = 1000$, $c = 1$, $\gamma_u = \gamma_v = 1$, stiffness ≈ 1000), and Table 2 shows results for the “Stingray saddle” ($a = 1$, $c = 100$, $\gamma_u = 1$, $\gamma_v = 101$, stiffness ≈ 100). The results indicate that Newton’s method is about 60 to 440 times faster than Min-Max Ascent, and that the Gradient Enhanced Min-Max method is about 2 to 3 times faster than Newton’s method and about 175 to 1000 times faster than Min-Max Ascent. These results are consistent with the results [7] for the Gradient Enhanced Newton (GEN) minimization method. When applied to Rosenbrock’s function, GEN is approximately 25 times faster than Newton’s method and approximately 2500 times faster than Steepest Descent.

In [8] we show that the Gradient Enhanced Min-Max method provides global asymptotic stability to the saddle point for functions such as the Stingray saddle function, which have a single proper stationary min-max point and satisfy a Lyapunov growth

Table 1: Banana saddle results ($a = 1000, c = 1$).

Method	Δt	$\ \dot{\mathbf{x}}(0)\ \Delta t$	Final t	# Steps	Ratio
Min-Max Ascent	10^{-6}	1.4999×10^{-3}	6.210995	6,210,995	980.2
Newton	10^{-3}	1.5133×10^{-3}	14.221	14221	2.24
GEMM	2.5×10^{-3}	1.4999×10^{-3}	15.84	6336	1

Table 2: Stingray saddle results ($a = 1, c = 100$).

Method	Δt	$\ \dot{\mathbf{x}}(0)\ \Delta t$	Final t	# Steps	Ratio
Min-Max Ascent	10^{-5}	1.2548×10^{-3}	7.32973	732,973	175.5
Newton	10^{-3}	1.2962×10^{-3}	11.74	11,740	2.81
GEMM	1.5×10^{-2}	1.2543×10^{-3}	62.625	4,175	1

condition. For the Stingray function Newton’s method is not stiff but does not provide global asymptotic stability. Min-Max Ascent, applied to the Stingray function, provides global asymptotic stability [8] but is very stiff. When applied to the Stingray function, the Gradient Enhanced Min-Max method is very fast and is not stiff, whereas Min-Max Ascent is very slow and very stiff. The Gradient Enhanced Min-Max method is approximately 3 times faster than Newton’s method and approximately 175 to 1000 times faster than Min-Max Ascent.

7 Min-Max Saddle Point with Equality Constraints

In this section we extend the results in [8] to the problem of finding Lagrangian saddle points $\mathbf{y} = (\mathbf{x}, \boldsymbol{\lambda})$ for the problem of minimizing a scalar-valued function $\phi(\mathbf{x})$ subject to equality constraints $\boldsymbol{\psi}(\mathbf{x}) = \mathbf{0}$. In particular we expand our previous results to handle the fact that $\mathcal{L}(\mathbf{x}, \boldsymbol{\lambda})$ is linear in $\boldsymbol{\lambda}$.

For the augmented Lagrangian \mathcal{L} , and its gradient $\mathbf{h}(\mathbf{y})$ and Hessian $\mathcal{H}(\mathbf{y})$ given by (19) and (25), respectively, we are particularly concerned with finding a **proper Lagrangian saddle point** $\mathbf{y}^* = (\mathbf{x}^*, \boldsymbol{\lambda}^*)$, at which:

- i) $\mathcal{L}(\mathbf{x}^*, \boldsymbol{\lambda}) \leq \mathcal{L}(\mathbf{x}^*, \boldsymbol{\lambda}^*) < \mathcal{L}(\mathbf{x}, \boldsymbol{\lambda}^*)$ for all $(\mathbf{x}, \boldsymbol{\lambda}) \neq (\mathbf{x}^*, \boldsymbol{\lambda}^*)$,
- ii) $\mathbf{h}^* = [\partial \mathcal{L}(\mathbf{y}^*) / \partial \mathbf{y}]^\top = \mathbf{0}$, where $\mathbf{h}(\mathbf{y}) = \nabla_{\mathbf{y}} \mathcal{L}(\mathbf{y})$,
- iii) $\mathcal{H}_{\mathbf{xx}}^* = \partial^2 \mathcal{L}(\mathbf{x}^*, \boldsymbol{\lambda}^*) / \partial \mathbf{x}^2 \geq 0$ (positive semidefinite),

where, for $\beta \geq 0$, the augmented Lagrangian is

$$\mathcal{L}(\mathbf{x}, \boldsymbol{\lambda}) = \phi(\mathbf{x}) - \boldsymbol{\lambda}^\top \boldsymbol{\psi}(\mathbf{x}) + \beta \frac{1}{2} \boldsymbol{\psi}^\top(\mathbf{x}) \boldsymbol{\psi}(\mathbf{x}). \tag{42}$$

In addition we assume that $\mathbf{h}(\mathbf{y}) = \nabla_{\mathbf{y}} \mathcal{L}(\mathbf{y}) = [\partial \mathcal{L}(\mathbf{y}) / \partial \mathbf{y}]^\top \neq \mathbf{0}$ for $\mathbf{y} \neq \mathbf{y}^*$ and that $\|\mathbf{h}(\mathbf{y})\| \rightarrow \infty$ as $\|\mathbf{y} - \mathbf{y}^*\| \rightarrow \infty$, where $\|\cdot\|$ denotes the Euclidian norm.

As a modification to Newton’s method (26) we consider a gradient transformation algorithm of the form

$$\dot{\mathbf{y}} = -\mathbf{P}(\mathbf{y}) \nabla_{\mathbf{y}} \mathcal{L}(\mathbf{y}) = -\mathcal{F}^{-1}(\mathbf{y}) \nabla_{\mathbf{y}} \mathcal{L}(\mathbf{y}), \tag{43}$$

where

$$\mathcal{F}(\mathbf{y}) = \mathcal{H}(\mathbf{y}) + \|\mathbf{h}\| \begin{bmatrix} \gamma_{\mathbf{x}} \mathbf{I}_n & \mathbf{0} \\ \mathbf{0} & -\gamma_{\boldsymbol{\lambda}} \mathbf{I}_m \end{bmatrix} = \begin{bmatrix} \gamma_{\mathbf{x}} \|\mathbf{h}\| \mathbf{I}_n + \frac{\partial^2 \mathcal{L}}{\partial \mathbf{x}^2} & -\boldsymbol{\Gamma}^\top \\ -\boldsymbol{\Gamma} & -\gamma_{\boldsymbol{\lambda}} \|\mathbf{h}\| \mathbf{I}_m \end{bmatrix}, \tag{44}$$

with

$$\mathbf{h}(\mathbf{y}) = \nabla_{\mathbf{y}}\mathcal{L}(\mathbf{y}) = \begin{bmatrix} \nabla_{\mathbf{x}}\mathcal{L} \\ \nabla_{\lambda}\mathcal{L} \end{bmatrix} = \begin{bmatrix} \left[\frac{\partial\mathcal{L}}{\partial\mathbf{x}} \right]^{\top} \\ -\psi \end{bmatrix}, \quad (45)$$

$$\mathcal{H}(\mathbf{y}) = \frac{\partial^2\mathcal{L}(\mathbf{y})}{\partial\mathbf{y}^2} = \begin{bmatrix} \mathcal{H}_{\mathbf{x}\mathbf{x}} & \mathcal{H}_{\lambda\mathbf{x}} \\ \mathcal{H}_{\lambda\mathbf{x}}^{\top} & \mathcal{H}_{\lambda\lambda} \end{bmatrix} = \begin{bmatrix} \frac{\partial^2\mathcal{L}}{\partial\mathbf{x}^2} & -\mathbf{\Gamma}^{\top} \\ -\mathbf{\Gamma} & \mathbf{0} \end{bmatrix}, \quad (46)$$

$$\mathbf{\Gamma} = \frac{\partial\psi}{\partial\mathbf{x}}. \quad (47)$$

7.1 Nonsingularity of $\mathcal{F}(\mathbf{y})$

We will show that for a sufficiently large constant $\gamma_{\mathbf{x}} \geq 0$ and any constant $\gamma_{\lambda} > 0$ the matrix $\mathcal{F}(\mathbf{y})$ in (44) is nonsingular for all \mathbf{y} . Hence the only equilibrium for (18) with (43)–(44) is at \mathbf{y}^* . To prove that $\mathcal{F}(\mathbf{y})$ is nonsingular, we have the following results:

Lemma 7.1 *For $\mathbf{y} \in \mathcal{R}^p$ let $\mathbf{M}(\mathbf{y})$ be an $s \times s$ matrix whose elements are functions of class C^q , $q \geq 0$, in a neighborhood of $\hat{\mathbf{y}} \in \mathcal{R}^p$, with distinct eigenvalues at $\hat{\mathbf{y}}$. Then the eigenvalues $\mu_k(\mathbf{y})$, $k = 1, \dots, s$, of $\mathbf{M}(\mathbf{y})$ are of class C^q in a neighborhood of $\hat{\mathbf{y}}$.*

Proof The characteristic equation is $0 = \mathcal{P}(\mu, \mathbf{y}) = |\mu\mathbf{I} - \mathbf{M}(\mathbf{y})| = \mu^s + p_{s-1}\mu^{s-1} + \dots + p_1\mu + p_0$, where \mathbf{I} denotes the $s \times s$ identity matrix. The coefficients $p_k(\mathbf{y})$ are C^q since they can be determined from Newton's identities [14, p. 227] in terms of the trace(\mathbf{M}^k), $k = 1, \dots, s$, of powers of $\mathbf{M}(\mathbf{y})$, which only involves products and sums of the elements of $\mathbf{M}(\mathbf{y})$. Then the lemma follows from the implicit function theorem [9, p. 21], with Jacobian $d\mathcal{P}(\mu_k, \hat{\mathbf{y}})/d\mu \neq 0$ for the case where the eigenvalues μ_k , $k = 1, \dots, s$, are distinct.

For repeated eigenvalues, the elements of $\mathbf{M}(\mathbf{y})$ can be perturbed by an arbitrarily small amount $\epsilon > 0$ to yield distinct eigenvalues [19, p. 89]. For a more detailed analysis of the case of repeated eigenvalues, see [20, p. 134]. Henceforth, we will consider only the case of distinct eigenvalues.

Theorem 7.1 *For $\mathbf{y} \in \mathcal{R}^p$ let $\mathbf{M}(\mathbf{y}) \in \mathcal{R}^{s \times s}$ be a continuous symmetric matrix with $\mathbf{M}(\mathbf{y}^*) \geq 0$ (≤ 0) and let $\mathcal{L}(\mathbf{y})$ be a scalar-valued function of class C^q , $q \geq 1$. Let $\mathbf{h}(\mathbf{y}) = [\partial\mathcal{L}/\partial\mathbf{y}]^{\top}$. If $\mathbf{h}(\mathbf{y}^*) = \mathbf{0}$, with $\mathbf{h}(\mathbf{y}) \neq \mathbf{0}$ for $\mathbf{y} \neq \mathbf{y}^*$ and $\|\mathbf{h}(\mathbf{y})\| \rightarrow \infty$ as $\|\mathbf{y} - \mathbf{y}^*\| \rightarrow \infty$, then for $\gamma \geq 0$ (≤ 0) with $|\gamma|$ sufficiently large, the $s \times s$ matrix $\mathbf{N}(\mathbf{y}) = \gamma\|\mathbf{h}(\mathbf{y})\|\mathbf{I} + \mathbf{M}(\mathbf{y})$ is positive definite (negative definite) for all $\mathbf{y} \neq \mathbf{y}^*$.*

Proof We consider the positive semidefinite case for $\mathbf{M}(\mathbf{y}^*)$. The proof for the negative semidefinite case is analogous. At \mathbf{y} let $\mu(\mathbf{y})$ denote the smallest (possibly negative) eigenvalue of $\mathbf{M}(\mathbf{y})$, with corresponding unit eigenvector $\boldsymbol{\xi}(\mathbf{y})$. For $\gamma \geq 0$ let $\omega(\mathbf{y}) = \mu(\mathbf{y}) + \gamma\|\mathbf{h}(\mathbf{y})\|$ denote the corresponding smallest eigenvalue of $\mathbf{N}(\mathbf{y})$, with corresponding unit eigenvector $\boldsymbol{\xi}(\mathbf{y})$, where $\boldsymbol{\xi}^{\top}\mathbf{N}(\mathbf{y})\boldsymbol{\xi} = \omega(\mathbf{y})\boldsymbol{\xi}^{\top}\boldsymbol{\xi} = \omega(\mathbf{y}) = \mu(\mathbf{y}) + \gamma\|\mathbf{h}(\mathbf{y})\|$. Let $\mathcal{B}_r = \{\mathbf{y} : \|\mathbf{y} - \mathbf{y}^*\| \leq r\}$. From Lemma 7.1 $\mu(\mathbf{y})$ is continuous on \mathcal{R}^p , with $\mu(\mathbf{y}^*) \geq 0$ and all the other eigenvalues of $\mathbf{M}(\mathbf{y}^*)$ are positive. For arbitrarily small $\epsilon > 0$ let $\bar{\mathbf{y}}$ be a minimal point for $\mu(\mathbf{y})$ on \mathcal{B}_ϵ . If $\bar{\mathbf{y}} = \mathbf{y}^*$ choose any $\bar{\gamma} > 0$. If $\bar{\mathbf{y}} \neq \mathbf{y}^*$ choose $\bar{\gamma} > \max\{0, -\mu(\bar{\mathbf{y}})/\|\mathbf{h}(\bar{\mathbf{y}})\|\}$. Then for $\gamma > \bar{\gamma}$, $\mu(\mathbf{y}) > 0 \forall \mathbf{y} \in \mathcal{B}_\epsilon - \{\mathbf{y}^*\}$.

For any $r \geq \epsilon$ let $\mathcal{X}_r = \{\mathbf{y} : \epsilon \leq \|\mathbf{y} - \mathbf{y}^*\| \leq r\}$, with $\|\mathbf{h}(\mathbf{y})\| > 0 \forall \mathbf{y} \in \mathcal{X}_r$. From the theorem of Weierstrass $\mu(\mathbf{y})/\|\mathbf{h}(\mathbf{y})\|$ takes on a minimum value at some point $\hat{\mathbf{y}} \in \mathcal{X}_r$. Let $\hat{\gamma}(r) = \max\{0, -\mu(\hat{\mathbf{y}})/\|\mathbf{h}(\hat{\mathbf{y}})\|\} \geq 0$. Then for $\gamma > \hat{\gamma}(r)$ we have $\omega(\mathbf{y})/\|\mathbf{h}(\mathbf{y})\| = \gamma + \mu(\mathbf{y})/\|\mathbf{h}(\mathbf{y})\| \geq \gamma + \mu(\hat{\mathbf{y}})/\|\mathbf{h}(\hat{\mathbf{y}})\| \geq \gamma - \hat{\gamma}(r) > 0 \forall \mathbf{y} \in \mathcal{X}_r$. The conditions on $\mathbf{h}(\mathbf{y})$ ensure that $\|\mathbf{h}(\mathbf{y})\| \not\rightarrow 0$ as $\|\mathbf{y} - \mathbf{y}^*\| \rightarrow \infty$. Thus $\hat{\gamma} = \lim_{r \rightarrow \infty} \{\hat{\gamma}(r)\}$ exists. Then $\omega(\mathbf{y}) > 0 \forall \mathbf{y} \neq \mathbf{y}^*$ provided $\gamma > \max(\bar{\gamma}, \hat{\gamma})$.

Lemma 7.2 *Let $\mathbf{A} \in \mathcal{R}^{n \times n}$ be symmetric and $\mathbf{B} \in \mathcal{R}^{n \times m}$. If \mathbf{A} is positive definite ($\mathbf{A} > 0$) then $\mathbf{B}^T \mathbf{A} \mathbf{B}$ is at least positive semidefinite ($\mathbf{B}^T \mathbf{A} \mathbf{B} \geq 0$).*

Proof For $\mathbf{z} \in \mathcal{R}^m$ and $\mathbf{s} \in \mathcal{R}^n$, let $\mathbf{s} = \mathbf{Bz}$. Then $\mathbf{s}^T \mathbf{A} \mathbf{s} > 0$ for $\mathbf{s} \neq \mathbf{0}$. Hence $\mathbf{z}^T \mathbf{B}^T \mathbf{A} \mathbf{Bz} \geq 0$ for $\mathbf{z} \neq \mathbf{0}$.

Lemma 7.3 *Let $\mathbf{A} \in \mathcal{R}^{n \times n}$ be symmetric and $\mathbf{B} \in \mathcal{R}^{n \times n}$. If $\mathbf{A} > 0$ (< 0) and $\mathbf{B} \geq 0$ (≤ 0) then $\mathbf{A} + \mathbf{B} > 0$ (< 0).*

Proof For $\mathbf{s} \in \mathcal{R}^n$ we have $\mathbf{s}^T (\mathbf{A} + \mathbf{B}) \mathbf{s} = \mathbf{s}^T \mathbf{A} \mathbf{s} + \mathbf{s}^T \mathbf{B} \mathbf{s} > 0$ (< 0) for all $\mathbf{s} \neq \mathbf{0}$.

Theorem 7.2 *For $\mathbf{A} \in \mathcal{R}^{n \times n}$ symmetric, $\mathbf{B} \in \mathcal{R}^{n \times m}$, and $\mathbf{D} \in \mathcal{R}^{m \times m}$ symmetric, the matrix*

$$\mathcal{F} = \begin{bmatrix} \mathbf{A} & \mathbf{B} \\ \mathbf{B}^T & \mathbf{D} \end{bmatrix}$$

is nonsingular, with $|\mathcal{F}| < 0$, if $\mathbf{A} > 0$ and $\mathbf{D} < 0$ (or if $\mathbf{A} < 0$ and $\mathbf{D} > 0$).

Proof Pre-multiplying the first block row by $\mathbf{B}^T \mathbf{A}^{-1}$ and subtracting from the second block row yields

$$|\mathcal{F}| = \begin{vmatrix} \mathbf{A} & \mathbf{B} \\ \mathbf{0} & \mathbf{D} - \mathbf{B}^T \mathbf{A}^{-1} \mathbf{B} \end{vmatrix} = |\mathbf{A}| |\mathbf{D} - \mathbf{B}^T \mathbf{A}^{-1} \mathbf{B}|.$$

For $\mathbf{A} > 0$, we have [21, p. 128] $|\mathbf{A}| = \mu_1 \cdots \mu_n > 0$, where $\mu_k, k = 1, \dots, n$, are the eigenvalues of \mathbf{A} . From Lemma 7.2 $\mathbf{B}^T \mathbf{A}^{-1} \mathbf{B} \geq 0$. Thus from Lemma 7.3 with $\mathbf{D} < 0$ we have $\mathbf{D} - \mathbf{B}^T \mathbf{A}^{-1} \mathbf{B} < 0$. Hence $|\mathbf{D} - \mathbf{B}^T \mathbf{A}^{-1} \mathbf{B}| = \omega_1 \cdots \omega_m < 0$, where $\omega_j, j = 1, \dots, m$, are the eigenvalues of $\mathbf{D} - \mathbf{B}^T \mathbf{A}^{-1} \mathbf{B}$. Thus, $|\mathcal{F}| = \mu_1 \cdots \mu_n \omega_1 \cdots \omega_m < 0$.

Theorem 7.3 *If $\mathbf{y}^* = (\mathbf{x}^*, \boldsymbol{\lambda}^*)$ is a proper Lagrangian $\max_{\boldsymbol{\lambda}} - \min_{\mathbf{x}}$ saddle point for a scalar-valued C^2 function*

$$\mathcal{L}(\mathbf{x}, \boldsymbol{\lambda}) = \phi(\mathbf{x}) - \boldsymbol{\lambda}^T \boldsymbol{\psi}(\mathbf{x}) + \frac{1}{2} \beta \boldsymbol{\psi}^T(\mathbf{x}) \boldsymbol{\psi}(\mathbf{x}),$$

with $\mathbf{h}(\mathbf{x}, \boldsymbol{\lambda}) = [\partial \mathcal{L} / \partial \mathbf{x}, \partial \mathcal{L} / \partial \boldsymbol{\lambda}]^T \neq \mathbf{0}$ for $\mathbf{y} \neq \mathbf{y}^$ and $\|\mathbf{h}(\mathbf{y})\| \rightarrow \infty$ as $\|\mathbf{y} - \mathbf{y}^*\| \rightarrow \infty$, and with*

$$\mathcal{H}(\mathbf{y}) = \frac{\partial^2 \mathcal{L}(\mathbf{y})}{\partial \mathbf{y}^2} = \begin{bmatrix} \mathcal{H}_{\mathbf{x}\mathbf{x}} & \mathcal{H}_{\mathbf{x}\boldsymbol{\lambda}} \\ \mathcal{H}_{\mathbf{x}\boldsymbol{\lambda}}^T & \mathcal{H}_{\boldsymbol{\lambda}\boldsymbol{\lambda}} \end{bmatrix},$$

then for sufficiently large $\gamma_{\mathbf{x}} \geq 0$ and any $\gamma_{\boldsymbol{\lambda}} > 0$ the matrix

$$\mathcal{F} = \begin{bmatrix} \gamma_{\mathbf{x}} \|\mathbf{h}\| \mathbf{I}_n + \mathcal{H}_{\mathbf{x}\mathbf{x}} & \mathcal{H}_{\mathbf{x}\boldsymbol{\lambda}} \\ \mathcal{H}_{\mathbf{x}\boldsymbol{\lambda}}^T & -\gamma_{\boldsymbol{\lambda}} \|\mathbf{h}\| \mathbf{I}_m \end{bmatrix}$$

is nonsingular, with $|\mathcal{F}| < 0$, for all $\mathbf{y} \neq \mathbf{y}^$.*

Proof From Theorem 7.1, for $\mathbf{y} \neq \mathbf{y}^*$, $\gamma_{\mathbf{x}} \|\mathbf{h}\| \mathbf{I}_n + \mathcal{H}_{\mathbf{x}\mathbf{x}} > 0$ for sufficiently large $\gamma_{\mathbf{x}} \geq 0$ and $-\gamma_{\boldsymbol{\lambda}} \|\mathbf{h}\| \mathbf{I}_m < 0$ for any $\gamma_{\boldsymbol{\lambda}} > 0$. Then $|\mathcal{F}| < 0$ follows from Theorem 7.2 with $\mathbf{A} = \gamma_{\mathbf{x}} \|\mathbf{h}\| \mathbf{I}_n + \mathcal{H}_{\mathbf{x}\mathbf{x}}$, $\mathbf{B} = \mathcal{H}_{\mathbf{x}\boldsymbol{\lambda}}$, and $\mathbf{D} = -\gamma_{\boldsymbol{\lambda}} \|\mathbf{h}\| \mathbf{I}_m$.

7.2 Speed of GEMM

Using \mathcal{F} from (44) write the GEMM algorithm in the form

$$\left\{ \|\mathbf{h}\| \begin{bmatrix} \gamma_{\mathbf{x}} \mathbf{I}_n & \mathbf{0} \\ \mathbf{0} & -\gamma_{\lambda} \mathbf{I}_m \end{bmatrix} + \begin{bmatrix} \frac{\partial^2 \mathcal{L}}{\partial \mathbf{x}^2} & -\Gamma^T \\ -\Gamma & \mathbf{0} \end{bmatrix} \right\} \begin{bmatrix} \dot{\mathbf{x}} \\ \dot{\lambda} \end{bmatrix} = - \begin{bmatrix} \nabla_{\mathbf{x}} \mathcal{L} \\ \nabla_{\lambda} \mathcal{L} \end{bmatrix}. \quad (48)$$

Thus, using (45), (27), and (28), we have

$$\|\mathbf{h}\| \begin{bmatrix} \gamma_{\mathbf{x}} \mathbf{I}_n & \mathbf{0} \\ \mathbf{0} & -\gamma_{\lambda} \mathbf{I}_m \end{bmatrix} \begin{bmatrix} \dot{\mathbf{x}} \\ \dot{\lambda} \end{bmatrix} + \frac{d\mathbf{h}}{dt} = -\mathbf{h}.$$

For small $\|\mathbf{h}\|$ or small $\gamma_{\mathbf{x}}, \gamma_{\lambda}$ GEMM approaches Newton's method applied to \mathcal{L} . For large $\|\mathbf{h}\|$ or large $\gamma_{\mathbf{x}}, \gamma_{\lambda}$ GEMM approaches Hestenes's Method of Multipliers applied to $\mathcal{L}/(\gamma_{\mathbf{x}} \|\mathbf{h}\|)$ with $\beta \rightarrow \gamma_{\mathbf{x}}/\gamma_{\lambda}$, that is,

$$\|\mathbf{h}\| \begin{bmatrix} \gamma_{\mathbf{x}} \mathbf{I}_n & \mathbf{0} \\ \mathbf{0} & -\gamma_{\lambda} \mathbf{I}_m \end{bmatrix} \begin{bmatrix} \dot{\mathbf{x}} \\ \dot{\lambda} \end{bmatrix} \approx -\mathbf{h}$$

yields

$$\begin{bmatrix} \dot{\mathbf{x}} \\ \dot{\lambda} \end{bmatrix} \approx - \begin{bmatrix} \frac{1}{\gamma_{\mathbf{x}}} \mathbf{I}_n & \mathbf{0} \\ \mathbf{0} & -\frac{1}{\gamma_{\lambda}} \mathbf{I}_m \end{bmatrix} \frac{1}{\|\mathbf{h}\|} \mathbf{h} = \frac{1}{\|\mathbf{h}\|} \begin{bmatrix} -\frac{1}{\gamma_{\mathbf{x}}} \nabla_{\mathbf{x}} \mathcal{L} \\ \frac{1}{\gamma_{\lambda}} \nabla_{\lambda} \mathcal{L} \end{bmatrix}$$

with "speed"

$$\|\dot{\mathbf{y}}\| \rightarrow \begin{cases} 1/\gamma & \text{if } \gamma_{\mathbf{x}} = \gamma_{\lambda} = \gamma, \\ 1/\gamma_{\mathbf{x}} & \text{if } \gamma_{\mathbf{x}} \ll \gamma_{\lambda}, \\ 1/\gamma_{\lambda} & \text{if } \gamma_{\lambda} \ll \gamma_{\mathbf{x}}, \end{cases}$$

for large $\|\mathbf{h}\|$, $\gamma_{\mathbf{x}}$, or γ_{λ} .

7.3 Stability of GEMM

For $\dot{\mathbf{y}} = \mathcal{F}^{-1} \mathbf{h}$ the only equilibrium is at $\mathbf{h} = \nabla_{\mathbf{y}} \mathcal{L} = \mathbf{0}$. As $\|\mathbf{h}\| \rightarrow 0$ GEMM approaches Newton's method ($\mathcal{F} \rightarrow \mathcal{H}$). Thus \mathbf{y}^* is at least locally asymptotically stable and non-stiff, with all eigenvalues $\mu = -1$. From Theorem 7.3 $\mathcal{F}^{-1}(\mathbf{y})$ exists for all \mathbf{y} , provided $\gamma_{\lambda} > 0$ and $\gamma_{\mathbf{x}} \geq 0$ is sufficiently large. Therefore the domain of attraction is all of \mathcal{R}^p and GEMM is globally asymptotically stable to \mathbf{y}^* .

8 Rosenbrock's Function with Constraint

As an Example we consider the problem of minimizing Rosenbrock's function

$$\phi(\mathbf{x}) = 100(x_1^2 - x_2)^2 + (1 - x_1)^2, \quad (49)$$

subject to the parabolic constraint

$$\psi(\mathbf{x}) = (x_1 - 2)^2 + x_2 - 1 = 0. \quad (50)$$

Figure 8 shows contours of constant $\phi(\mathbf{x})$, along with the constraint $\psi(\mathbf{x}) = 0$.

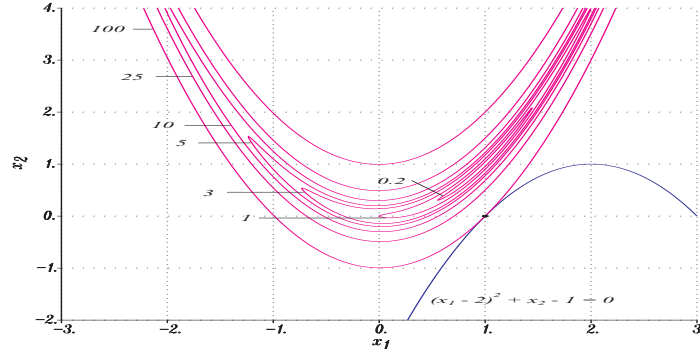


Figure 8: Rosenbrock’s function with parabolic constraint.

The gradient and the Hessian matrix of ϕ are given by

$$\nabla\phi(\mathbf{x}) = \left[\frac{\partial\phi}{\partial\mathbf{x}} \right]^\top = \begin{bmatrix} 400x_1(x_1^2 - x_2) + 2(x_1 - 1) \\ -200(x_1^2 - x_2) \end{bmatrix}, \tag{51}$$

$$\nabla^2\phi(\mathbf{x}) = \frac{\partial^2\phi}{\partial\mathbf{x}^2} = \begin{bmatrix} 1200x_1^2 - 400x_2 + 2 & -400x_1 \\ -400x_1 & 400 \end{bmatrix}. \tag{52}$$

Rosenbrock’s function ϕ is analogous to a curved canyon with very steep walls and a shallow sloping parabolic valley floor, defined by $x_2 = x_1^2$. The function has a single proper unconstrained global minimum at $\hat{\mathbf{x}} = [1, 1]^\top$, with $\phi(\mathbf{x}) > 0$ for all $\mathbf{x} \neq \hat{\mathbf{x}}$. Note that $\nabla\phi(\mathbf{x}) \neq \mathbf{0}$ except at $\hat{\mathbf{x}}$ and $\|\nabla\phi(\mathbf{x})\| \rightarrow \infty$ as $\|\mathbf{x} - \hat{\mathbf{x}}\| \rightarrow \infty$. Hence contours of constant ϕ are topologically equivalent to spheres [14, p. 215]. On the other hand, $\phi(\mathbf{x})$ is not a convex function, that is, it does not satisfy $\phi[\theta\mathbf{x}_1 + (1 - \theta)\mathbf{x}_2] \leq \theta\phi(\mathbf{x}_1) + (1 - \theta)\phi(\mathbf{x}_2)$ for all $\mathbf{x}_1, \mathbf{x}_2$, and $0 \leq \theta \leq 1$. This follows [17, p. 425] from the fact that $\nabla^2\phi(\mathbf{x})$ is positive definite only in the region $x_2 < x_1^2 + 1/2$. Some numerical optimization algorithms have trouble with Rosenbrock’s function because they exhibit “stiff” dynamics. For example, applied to the unconstrained problem, the discrete version of Steepest Descent “chatters” along the valley floor.

For the constrained optimization problem the augmented Lagrangian is

$$\begin{aligned} \mathcal{L} &= \phi - \lambda\psi + \frac{1}{2}\beta\psi^2 \\ &= 100(x_1^2 - x_2)^2 + (1 - x_1)^2 - \lambda \left[(x_1 - 2)^2 + x_2 - 1 \right] \\ &\quad + \frac{1}{2}\beta \left[(x_1 - 2)^2 + x_2 - 1 \right]^2. \end{aligned}$$

With $\mathbf{y}^\top = [\mathbf{x}^\top, \lambda]$, the gradient of \mathcal{L} is

$$\begin{aligned} \nabla_{\mathbf{y}} \mathcal{L} &= \left[\frac{\partial \mathcal{L}}{\partial \mathbf{y}} \right]^\top = \begin{bmatrix} \frac{\partial \mathcal{L}}{\partial x_1} \\ \frac{\partial \mathcal{L}}{\partial x_2} \\ \frac{\partial \mathcal{L}}{\partial \lambda} \end{bmatrix} = \begin{bmatrix} \frac{\partial \phi}{\partial x_1} + (\beta\psi - \lambda) \frac{\partial \psi}{\partial x_1} \\ \frac{\partial \phi}{\partial x_2} + (\beta\psi - \lambda) \frac{\partial \psi}{\partial x_2} \\ -\psi \end{bmatrix} \\ &= \begin{bmatrix} 400(x_1^2 - x_2)x_1 - 2(1 - x_1) + \left(\beta \left[(x_1 - 2)^2 + (x_2 - 1) \right] - \lambda \right) 2(x_1 - 2) \\ -200(x_1^2 - x_2) + \left(\beta \left[(x_1 - 2)^2 + (x_2 - 1) \right] - \lambda \right) \\ -(x_1 - 2)^2 - x_2 + 1 \end{bmatrix} \end{aligned} \quad (53)$$

and the Hessian of \mathcal{L} is

$$\mathcal{H} \triangleq \nabla_{\mathbf{y}}^2 \mathcal{L} = \frac{\partial^2 \mathcal{L}}{\partial \mathbf{y}^2} = \begin{bmatrix} \frac{\partial^2 \mathcal{L}}{\partial \mathbf{x}^2} & - \left[\frac{\partial \psi}{\partial \mathbf{x}} \right]^\top \\ - \frac{\partial \psi}{\partial \mathbf{x}} & 0 \end{bmatrix} = [\mathcal{H}_{ij}], \quad (54)$$

where

$$\begin{aligned} \mathcal{H}_{11} &= \frac{\partial^2 \mathcal{L}}{\partial x_1^2} = \frac{\partial^2 \phi}{\partial x_1^2} + (\beta\psi - \lambda) \frac{\partial^2 \psi}{\partial x_1^2} + \beta \left(\frac{\partial \psi}{\partial x_1} \right)^2 \\ &= 1200x_1^2 - 400x_2 + 2 + 2 \left(\beta \left[(x_1 - 2)^2 + (x_2 - 1) \right] - \lambda \right) + 4\beta (x_1 - 2)^2, \end{aligned} \quad (55)$$

$$\begin{aligned} \mathcal{H}_{12} = \mathcal{H}_{21} &= \frac{\partial^2 \mathcal{L}}{\partial x_1 \partial x_2} = \frac{\partial^2 \phi}{\partial x_1 \partial x_2} + (\beta\psi - \lambda) \frac{\partial^2 \psi}{\partial x_1 \partial x_2} + \beta \frac{\partial \psi}{\partial x_1} \frac{\partial \psi}{\partial x_2} \\ &= -400x_1 + 2\beta (x_1 - 2), \end{aligned} \quad (56)$$

$$\mathcal{H}_{13} = \mathcal{H}_{31} = \frac{\partial^2 \mathcal{L}}{\partial x_1 \partial \lambda} = -\frac{\partial \psi}{\partial x_1} = -2(x_1 - 2), \quad (57)$$

$$\mathcal{H}_{22} = \frac{\partial^2 \mathcal{L}}{\partial x_2^2} = \frac{\partial^2 \phi}{\partial x_2^2} + (\beta\psi - \lambda) \frac{\partial^2 \psi}{\partial x_2^2} + \beta \left(\frac{\partial \psi}{\partial x_2} \right)^2 = 200 + \beta, \quad (58)$$

$$\mathcal{H}_{23} = \mathcal{H}_{32} = \frac{\partial^2 \mathcal{L}}{\partial x_2 \partial \lambda} = -\frac{\partial \psi}{\partial x_2} = -1, \quad (59)$$

$$\mathcal{H}_{33} = \frac{\partial^2 \mathcal{L}}{\partial \lambda^2} = 0. \quad (60)$$

The first-order necessary conditions for $\max_{\lambda} \min_{\mathbf{x}} \mathcal{L}(\mathbf{x}, \lambda, \beta)$ are:

$$\begin{aligned} 0 &= \frac{\partial \mathcal{L}}{\partial x_1} = 400(x_1^2 - x_2)x_1 - 2(1 - x_1) - 2\lambda (x_1 - 2) \\ &\quad + \beta \left[(x_1 - 2)^2 + x_2 - 1 \right] 2(x_1 - 2), \end{aligned} \quad (61)$$

$$0 = \frac{\partial \mathcal{L}}{\partial x_2} = -200(x_1^2 - x_2) - \lambda + \beta \left[(x_1 - 2)^2 + x_2 - 1 \right], \quad (62)$$

$$0 = \frac{\partial \mathcal{L}}{\partial \lambda} = -\psi = -(x_1 - 2)^2 - x_2 + 1. \quad (63)$$

At $(\mathbf{x}, \lambda) = (\mathbf{x}^*, \lambda^*)$, with Lagrangian $L(\mathbf{x}, \lambda) = \mathcal{L}(\mathbf{x}, \lambda, \beta)|_{\beta=0}$, using (63) in (62) with $\beta = 0$ yields

$$\lambda = -200 \left\{ x_1^2 + \left[(x_1 - 2)^2 - 1 \right] \right\}. \tag{64}$$

Then using (63) and (64) in (61) yields

$$0 = \frac{\partial L}{\partial x_1} = 800x_1^3 - 2400x_1^2 + 2801x_1 - 1201.$$

This cubic polynomial has roots $x_1 = 1, 1 \pm \frac{1}{40}i\sqrt{802}$.

Thus the unique constrained global minimal point is

$$\mathbf{y}^* = (x_1^*, x_2^*, \lambda^*) = (1, 0, -200), \tag{65}$$

with $\phi^* = \phi(\mathbf{x}^*) = 100$ and $\psi^* = \psi(\mathbf{x}^*) = 0$, at which $\nabla_{\mathbf{y}}L(\mathbf{x}^*, \lambda^*) = \nabla_{\mathbf{y}}\mathcal{L}(\mathbf{x}^*, \lambda^*, \beta) = \mathbf{0}$, with

$$\nabla_{\mathbf{x}}L(\mathbf{y}) \neq \mathbf{0} \text{ and } \nabla_{\mathbf{y}}\mathcal{L}(\mathbf{y}) \neq \mathbf{0} \text{ for } \mathbf{y} \neq \mathbf{y}^* \tag{66}$$

and

$$\|\nabla_{\mathbf{x}}L(\mathbf{y})\| \rightarrow \infty \text{ and } \|\nabla_{\mathbf{y}}\mathcal{L}(\mathbf{y})\| \rightarrow \infty \text{ as } \|\mathbf{y} - \mathbf{y}^*\| \rightarrow \infty \tag{67}$$

for all $\beta \geq 0$.

Note that at \mathbf{y}^* the Hessian matrix (12) for the Lagrangian L ,

$$H(\mathbf{y}^*) = \frac{\partial^2 L(\mathbf{x}^*, \lambda^*)}{\partial \mathbf{x}^2} = \begin{bmatrix} 1602 & -400 \\ -400 & 200 \end{bmatrix} \tag{68}$$

is positive definite. Thus the second-order sufficient condition (6) is satisfied by the stronger condition that $H(\mathbf{x}^*, \lambda^*)$ is positive definite. For this Example switching from $\max_{\lambda} \min_{\mathbf{x}} L(\mathbf{x}, \lambda)$ to $\max_{\lambda} \min_{\mathbf{x}} \mathcal{L}(\mathbf{x}, \lambda, \beta)$ is not mandatory. However, we will continue using $\mathcal{L}(\mathbf{x}, \lambda, \beta)$, with $L(\mathbf{x}, \lambda) = \mathcal{L}(\mathbf{x}, \lambda, 0)$.

9 Augmented Lagrangian Trajectory Following

9.1 Min-max ascent

Choosing

$$\mathbf{P} = \begin{bmatrix} \mathbf{P}_{\mathbf{x}\mathbf{x}} & \mathbf{P}_{\mathbf{x}\lambda} \\ \mathbf{P}_{\lambda\mathbf{x}} & \mathbf{P}_{\lambda\lambda} \end{bmatrix} = \begin{bmatrix} \mathbf{I}_n & \mathbf{0} \\ \mathbf{0} & -\mathbf{I}_m \end{bmatrix} \tag{69}$$

in (20) yields

$$\dot{\mathbf{x}} = -\nabla_{\mathbf{x}}\mathcal{L} = -\nabla\phi + \mathbf{\Gamma}^T [\boldsymbol{\lambda} - \beta\boldsymbol{\psi}], \tag{70}$$

$$\dot{\boldsymbol{\lambda}} = \nabla_{\lambda}\mathcal{L} = -\boldsymbol{\psi}, \tag{71}$$

which corresponds to steepest descent for \mathbf{x} on $\mathcal{L}(\mathbf{x}, \boldsymbol{\lambda}, \beta)$ and steepest ascent for $\boldsymbol{\lambda}$ on $\mathcal{L}(\mathbf{x}, \boldsymbol{\lambda}, \beta)$. We will set $\beta = 0$, yielding the Min-Max Ascent algorithm considered in [3].

9.1.1 Simulation results

For the Example problem in Section 8 the Min-Max Ascent equations of motion are

$$\begin{aligned}\dot{x}_1 &= -400(x_1^2 - x_2)x_1 + 2(1 - x_1) + \left(\lambda - \beta \left((x_1 - 2)^2 + (x_2 - 1)\right)\right) 2(x_1 - 2), \\ \dot{x}_2 &= 200(x_1^2 - x_2) + \left(\lambda - \beta \left((x_1 - 2)^2 + (x_2 - 1)\right)\right), \\ \dot{\lambda} &= -(x_1 - 2)^2 - x_2 + 1.\end{aligned}\tag{72}$$

The state perturbation equations $\dot{\boldsymbol{\eta}} = \mathbf{A}\boldsymbol{\eta}$ are

$$\begin{bmatrix} \dot{\boldsymbol{\eta}}_{\mathbf{x}} \\ \dot{\boldsymbol{\eta}}_{\mathbf{y}} \end{bmatrix} = \begin{bmatrix} -\frac{\partial^2 \mathcal{L}}{\partial \mathbf{x}^2} & -\frac{\partial^2 \mathcal{L}}{\partial \mathbf{x} \partial \boldsymbol{\lambda}} \\ \frac{\partial^2 \mathcal{L}}{\partial \boldsymbol{\lambda} \partial \mathbf{x}} & \frac{\partial^2 \mathcal{L}}{\partial \boldsymbol{\lambda}^2} \end{bmatrix} \begin{bmatrix} \boldsymbol{\eta}_{\mathbf{x}} \\ \boldsymbol{\eta}_{\mathbf{y}} \end{bmatrix}\tag{73}$$

and yield

$$\begin{bmatrix} \dot{\boldsymbol{\eta}}_1 \\ \dot{\boldsymbol{\eta}}_2 \\ \dot{\boldsymbol{\eta}}_3 \end{bmatrix} = \begin{bmatrix} a_{11} & 400x_1 - 2\beta(x_1 - 2) & 2(x_1 - 2) \\ 400x_1 - 2\beta(x_1 - 2) & -200 - \beta & 1 \\ -2(x_1 - 2) & -1 & 0 \end{bmatrix} \begin{bmatrix} \boldsymbol{\eta}_1 \\ \boldsymbol{\eta}_2 \\ \boldsymbol{\eta}_3 \end{bmatrix},$$

where

$$a_{11} = -1200x_1^2 + 400x_2 - 2 - 2\left(\beta \left((x_1 - 2)^2 + (x_2 - 1)\right) - \lambda\right) - 4\beta(x_1 - 2)^2.$$

At $(\mathbf{x}^*, \lambda^*) = (1, 0, -200)$

$$\begin{bmatrix} \dot{\boldsymbol{\eta}}_1 \\ \dot{\boldsymbol{\eta}}_2 \\ \dot{\boldsymbol{\eta}}_3 \end{bmatrix} = \begin{bmatrix} -1602 - 4\beta & 400 + 2\beta & -2 \\ 400 + 2\beta & -200 - \beta & 1 \\ 2 & -1 & 0 \end{bmatrix} \begin{bmatrix} \boldsymbol{\eta}_1 \\ \boldsymbol{\eta}_2 \\ \boldsymbol{\eta}_3 \end{bmatrix}.$$

For $\beta = 0$ the eigenvalues (μ_k) and eigenvectors $(\boldsymbol{\xi}_k)$ of \mathbf{A} are

$$\begin{aligned}\mu_1 &= -5.00 \times 10^{-3}, & \boldsymbol{\xi}_1^T &= [6.23 \times 10^{-8} \quad 5.00 \times 10^{-3} \quad 1.0], \\ \mu_2 &= -93.90, & \boldsymbol{\xi}_2^T &= [-0.256 \quad -0.967 \quad -4.83 \times 10^{-3}], \\ \mu_3 &= -1708.09, & \boldsymbol{\xi}_3^T &= [-0.967 \quad 0.256 \quad 1.28 \times 10^{-3}].\end{aligned}\tag{74}$$

The Lyapunov exponents are $(\sigma_1, \sigma_2, \sigma_3) = (\mu_1, \mu_2, \mu_3)$. This is a very stiff system, with “stiffness” $\Sigma \triangleq |\sigma_{\max} - \sigma_{\min}| \approx 1,700$.

Figure 9 shows Min-Max Ascent trajectories for $\lambda(0) = 0$ and $\beta = 0$, starting from initial $\mathbf{x}(0)$ at the edges of the plot region. The trajectories were generated using standard 4-*th* order Runge-Kutta integration with a fixed step size $\Delta t = 2 \times 10^{-4}$. The trajectories in Figure 9 rapidly approach the valley of Rosenbrock’s function then move more slowly along the valley until they reach a region just below the unconstrained minimal point $\hat{\mathbf{x}} = (1, 1)$. Then they move agonizingly slowly down to the constrained minimal point $\mathbf{x}^* = (1, 0)$. For example, the trajectory from $\mathbf{y}(0) = (-2, 4, 0)$ takes approximately 0.1 sec. of simulation time to reach the valley, approximately 3 sec. more to reach a neighborhood

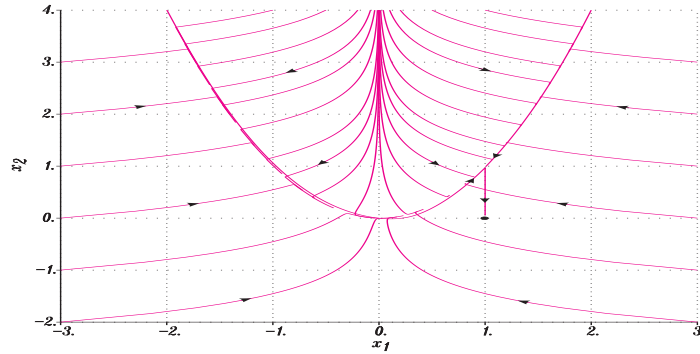


Figure 9: Min-Max Ascent ($\lambda(0) = 0, \beta = 0$).

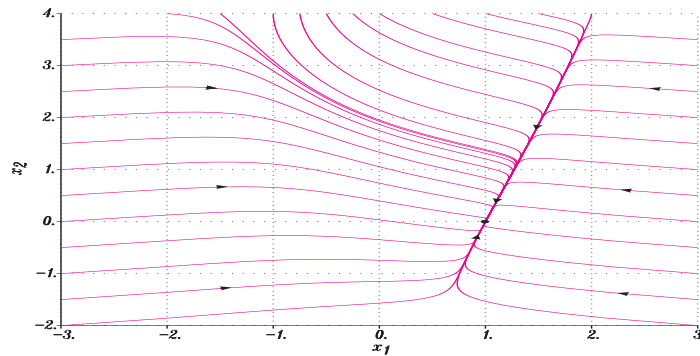


Figure 10: Min-Max Ascent ($\lambda(0) = \lambda^* = -200, \beta = 0$).

of $\hat{\mathbf{x}}$, and then more than 1300 sec. longer to converge to $\mathbf{y}^* = (1, 0, -200)$, at $t_f \approx 1400$ sec., with stopping criterion $\|\nabla_{\mathbf{y}} L\| \leq 10^{-3}$. All other trajectories, which are x_1, x_2 projections of the three-dimensional $\mathbf{y} = (x_1, x_2, \lambda)$ trajectories, behaved similarly and converged to \mathbf{y}^* , but for plotting purposes were terminated after $t = 0.1$ sec., to illustrate that they overshoot or undershoot the valley.

The extremely slow convergence is associated with λ [due to μ_1 in (74)] and is a result of the choice $\lambda(0) = 0$. The trajectories are essentially steepest descent on $\phi(\mathbf{x})$ until $\lambda(t)$ very slowly converges to λ^* . Figure 10 shows trajectories from the same initial conditions as in Figure 9, except with $\lambda(0) = \lambda^*$. All trajectories, with step size $\Delta t = 10^{-4}$, were terminated when $\|\nabla_{\mathbf{y}} L\| \leq 10^{-3}$, but only required a total of approximately 0.1 sec. of simulation time to converge to \mathbf{y}^* .

Figure 11 shows the Lyapunov exponent time histories for Min-Max Ascent on L , starting from $(x_1, x_2, \lambda) = (-2.5, 0, 0)$ with $\beta = 0$. The system is uniformly very stiff, with $\Sigma(t) = |\sigma_{\max}(t) - \sigma_{\min}(t)|$ varying between approximately 250 and 1,700 and converging to $\Sigma \approx 1,700$.

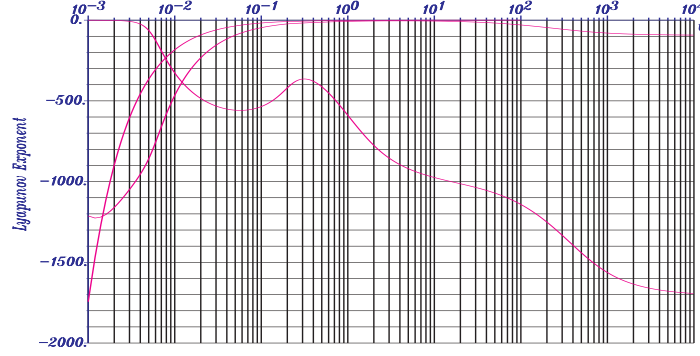


Figure 11: Lyapunov exponents for Min-Max Ascent ($\lambda(0) = 0$, $\beta = 0$).

9.1.2 Stability analysis

Lyapunov's first method establishes that the Min-Max Ascent system (72) is locally asymptotically stable to \mathbf{y}^* for $\beta = 0$. Alternatively, in [4] a min-max sufficiency condition is developed using

$$V(\mathbf{y}) = \frac{1}{2} [\mathbf{y} - \mathbf{y}^*]^\top [\mathbf{y} - \mathbf{y}^*] = \frac{1}{2} [\mathbf{x} - \mathbf{x}^*]^\top [\mathbf{x} - \mathbf{x}^*] + \frac{1}{2} [\boldsymbol{\lambda} - \boldsymbol{\lambda}^*]^\top [\boldsymbol{\lambda} - \boldsymbol{\lambda}^*]. \quad (75)$$

Along $\mathbf{y}(t)$

$$\dot{V}(\mathbf{y}) = \frac{\partial V}{\partial \mathbf{x}} \dot{\mathbf{x}} + \frac{\partial V}{\partial \boldsymbol{\lambda}} \dot{\boldsymbol{\lambda}} = -[\mathbf{x} - \mathbf{x}^*]^\top \nabla_{\mathbf{x}} \mathcal{L} + [\boldsymbol{\lambda} - \boldsymbol{\lambda}^*]^\top \nabla_{\boldsymbol{\lambda}} \mathcal{L}. \quad (76)$$

If

$$\dot{V}(\mathbf{y}) < 0 \quad \text{provided } \dot{\mathbf{y}} \neq \mathbf{0} \quad (77)$$

in a neighborhood of \mathbf{y}^* , then $V(\mathbf{y})$ is a Lyapunov function, establishing at least local asymptotic stability [14, p. 217]. The function (75), with $\beta = 0$ so $\mathcal{L} = L$, is used in [3] to establish local asymptotic stability of \mathbf{y}^* for Min-Max Ascent applied to finding a saddle point of $L(\mathbf{x}, \boldsymbol{\lambda})$ under the conditions that L is linear in $\boldsymbol{\lambda}$ and $H = \partial^2 L / \partial \mathbf{x}^2$ is positive definite at $(\mathbf{x}^*, \boldsymbol{\lambda}^*)$.

Unfortunately, for our Example the function (75) does not satisfy (77) everywhere and can not be used to establish global asymptotic stability for our Example. In fact, for some saddle-point problems, Min-Max Ascent can produce Hamiltonian systems [8], which can not be asymptotically stable. However, simulation experiments indicate that Min-Max Ascent is globally asymptotically stable to \mathbf{y}^* for our Example.

9.2 Hestenes' method of multipliers

Choosing

$$\mathbf{P} = \begin{bmatrix} \mathbf{P}_{\mathbf{x}\mathbf{x}} & \mathbf{P}_{\mathbf{x}\boldsymbol{\lambda}} \\ \mathbf{P}_{\boldsymbol{\lambda}\mathbf{x}} & \mathbf{P}_{\boldsymbol{\lambda}\boldsymbol{\lambda}} \end{bmatrix} = \begin{bmatrix} \mathbf{I}_n & \mathbf{0} \\ \mathbf{0} & -\beta \mathbf{I}_m \end{bmatrix} \quad (78)$$

in (20) yields

$$\dot{\mathbf{x}} = -\nabla_{\mathbf{x}} \mathcal{L} = -\nabla \phi + \mathbf{F}^\top [\boldsymbol{\lambda} - \beta \boldsymbol{\psi}], \quad (79)$$

$$\dot{\boldsymbol{\lambda}} = \nabla_{\boldsymbol{\lambda}} \mathcal{L} = -\beta \boldsymbol{\psi}, \quad (80)$$

corresponding to Hestenes’ Method of Multipliers [13].

For our Example the equations of motion for Hestenes’ Method of Multipliers are

$$\begin{aligned} \dot{x}_1 &= -400(x_1^2 - x_2)x_1 + 2(1 - x_1) + \left(\lambda - \beta \left((x_1 - 2)^2 + (x_2 - 1)\right)\right) 2(x_1 - 2), \\ \dot{x}_2 &= 200(x_1^2 - x_2) + \left(\lambda - \beta \left((x_1 - 2)^2 + (x_2 - 1)\right)\right), \\ \dot{\lambda} &= -\beta \left[(x_1 - 2)^2 + x_2 - 1\right]. \end{aligned}$$

The state perturbation equations are

$$\begin{bmatrix} \dot{\eta}_1 \\ \dot{\eta}_2 \\ \dot{\eta}_3 \end{bmatrix} = \begin{bmatrix} a_{11} & 400x_1 - 2\beta(x_1 - 2) & 2(x_1 - 2) \\ 400x_1 - 2\beta(x_1 - 2) & -200 - \beta & 1 \\ -2\beta(x_1 - 2) & -\beta & 0 \end{bmatrix} \begin{bmatrix} \eta_1 \\ \eta_2 \\ \eta_3 \end{bmatrix},$$

where

$$a_{11} = -1200x_1^2 + 400x_2 - 2 - 2 \left(\beta \left((x_1 - 2)^2 + (x_2 - 1)\right) - \lambda\right) - 4\beta(x_1 - 2)^2.$$

At $(\mathbf{x}^*, \lambda^*)$

$$\begin{bmatrix} \dot{\eta}_1 \\ \dot{\eta}_2 \\ \dot{\eta}_3 \end{bmatrix} = \begin{bmatrix} -1602 - 4\beta & 400 + 2\beta & -2 \\ 400 + 2\beta & -200 - \beta & 1 \\ 2\beta & -\beta & 0 \end{bmatrix} \begin{bmatrix} \eta_1 \\ \eta_2 \\ \eta_3 \end{bmatrix}.$$

For $\beta = 5$ the state perturbation equations have Lyapunov exponents $(\sigma_1, \sigma_2, \sigma_3)$ equal to the eigenvalues $(\mu_1, \mu_2, \mu_3) = (-2.44 \times 10^{-2}, -94.91, -1732.07)$. This is a very stiff system, with stiffness $\Sigma = |\sigma_{\max} - \sigma_{\min}| \approx 1,700$, which is approximately that of Min-Max Ascent. For $\beta = 100$ the eigenvalues are $(\mu_1, \mu_2, \mu_3) = (-0.33, -109.64, -2192.03)$, with stiffness $\Sigma = |\sigma_{\max} - \sigma_{\min}| \approx 2,200$. For very large β the state perturbation matrix

$$\mathbf{A} \approx \begin{bmatrix} -4\beta & 2\beta & -2 \\ 2\beta & -\beta & 1 \\ 2\beta & -\beta & 0 \end{bmatrix}$$

has eigenvalues $(\mu_1, \mu_2, \mu_3) = \left(0, -\frac{5}{2}\beta + \frac{1}{2}\sqrt{25\beta^2 - 20\beta}, -\frac{5}{2}\beta - \frac{1}{2}\sqrt{25\beta^2 - 20\beta}\right) \rightarrow (0, 0, -5\beta)$. Thus the stiffness increases with increasing β . However, as we shall show later, even for $\beta = 5$ the convergence for the Method of Multipliers is much faster than for Min-Max Ascent.

As with Min-Max Ascent, Lyapunov’s first method establishes local asymptotic stability of \mathbf{y}^* , but no suitable Lyapunov function is known to establish global asymptotic stability. However, experimental simulation results indicate that Hestenes’ Method of Multipliers is globally asymptotically stable for our Example.

Figure 12 shows trajectories for Hestenes’ Method of Multipliers applied to the augmented Lagrangian \mathcal{L} with $\lambda(0) = 0$ and $\beta = 5$, using step size $\Delta t = 10^{-4}$ with termination when $\|\nabla_{\mathbf{y}}\mathcal{L}\| \leq 10^{-3}$. The behavior is similar to Min-Max Ascent, except for faster convergence to the constrained minimum point, at approximately $t_f = 300$ sec.

Figure 13 shows the Lyapunov exponent time histories for Hestenes Method of Multipliers applied to \mathcal{L} , starting from $(x_1, x_2, \lambda) = (-2.5, 0, 0)$ with $\beta = 5$. The stiffness is similar to Min-Max Ascent, with $\Sigma(t)$ varying between approximately 100 and 1,700 and converging to $\Sigma \approx 1,700$.

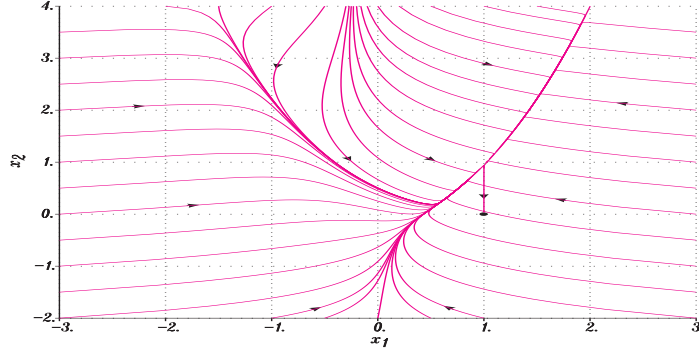


Figure 12: Method of Multipliers ($\lambda(0) = 0$, $\beta = 5$).

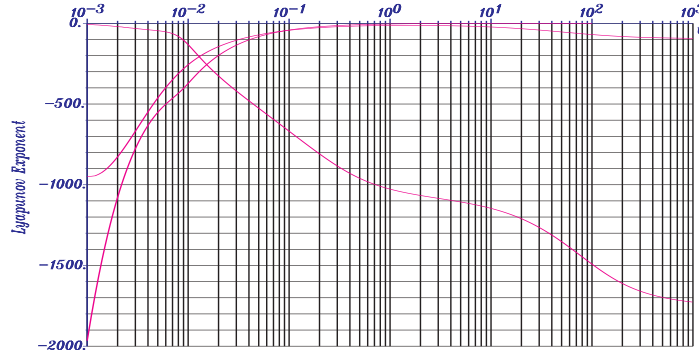


Figure 13: Method of Multipliers Lyapunov exponents ($\lambda(0) = 0$, $\beta = 5$).

9.3 Newton's method

Choosing

$$\mathbf{P} = \begin{bmatrix} \mathbf{P}_{\mathbf{x}\mathbf{x}} & \mathbf{P}_{\mathbf{x}\lambda} \\ \mathbf{P}_{\lambda\mathbf{x}} & \mathbf{P}_{\lambda\lambda} \end{bmatrix} = \mathcal{H}^{-1} = \begin{bmatrix} \frac{\partial^2 \mathcal{L}}{\partial \mathbf{x}^2} & -\mathbf{\Gamma}^\top \\ -\mathbf{\Gamma} & \mathbf{0} \end{bmatrix}^{-1}, \quad (81)$$

in (20), where $\mathbf{\Gamma} = \partial\psi/\partial\mathbf{x}$, yields Newton's method

$$\begin{bmatrix} \dot{\mathbf{x}} \\ \dot{\lambda} \end{bmatrix} = -\mathcal{H}^{-1}(\mathbf{y}) \begin{bmatrix} \nabla_{\mathbf{x}} \mathcal{L} \\ \nabla_{\lambda} \mathcal{L} \end{bmatrix} = -\mathcal{H}^{-1}(\mathbf{y}) \begin{bmatrix} \nabla_{\mathbf{x}} \mathcal{L} \\ -\psi \end{bmatrix}. \quad (82)$$

At the constrained minimal point the state perturbation equations (30) and (32) have $\mathbf{A}(\mathbf{y}^*) = -\mathbf{I}$, with eigenvalues $\mu = -1$, yielding a non stiff system.

For our Example problem,

$$\mathcal{H} = \begin{bmatrix} \mathcal{H}_{11} & -400x_1 + 2\beta(x_1 - 2) & -2(x_1 - 2) \\ -400x_1 + 2\beta(x_1 - 2) & 200 + \beta & -1 \\ -2(x_1 - 2) & -1 & 0 \end{bmatrix},$$

where

$$\mathcal{H}_{11} = 1200x_1^2 - 400x_2 + 2 + 2 \left(\beta \left((x_1 - 2)^2 + (x_2 - 1) \right) - \lambda \right) + 4\beta (x_1 - 2)^2.$$

Then

$$\mathbf{P} = \mathcal{H}^{-1} = \frac{1}{|\mathcal{H}|} \text{adj}(\mathcal{H}), \tag{83}$$

where

$$|\mathcal{H}| = - (3600 + 2\beta) x_1^2 + (6400 + 8\beta) x_1 + (400 - 2\beta) x_2 - 3202 - 6\beta + 2\lambda \tag{84}$$

and the adjugate matrix is

$$\text{adj}(\mathcal{H}) = \begin{bmatrix} -1 & 2(x_1 - 2) & 800(x_1 - 1) \\ 2(x_1 - 2) & -4(x_1 - 2)^2 & c_{23} \\ 800(x_1 - 1) & c_{32} & c_{33} \end{bmatrix} \tag{85}$$

with

$$\begin{aligned} c_{23} = c_{32} &= (2\beta + 2000) x_1^2 - (8\beta + 1600) x_1 + (2\beta - 400) x_2 + 2 + 6\beta - 2, \\ c_{33} &= (2\beta^2 + 4000\beta + 80\,000) x_1^2 - 8\beta(1000 + \beta) x_1 \\ &\quad + (2\beta^2 - 80\,000) x_2 + 6\beta^2 + 4402\beta - \lambda(400 + 2\beta) + 400. \end{aligned}$$

At points where $|\mathcal{H}| = 0$ the inverse \mathcal{H}^{-1} fails to exist. As a result, Newton’s method is not globally asymptotically stable to the solution point $(x_1^*, x_2^*, \lambda^*) = (1, 0, -200)$ for our Example problem. Specifically, we have $|\mathcal{H}| = 0$ on the parabola

$$(400 - 2\beta) x_2 = (3600 + 2\beta) x_1^2 - (6400 + 8\beta) x_1 + 3202 - 2\lambda + 6\beta.$$

At the optimal point $\mathbf{y}^* = (1, 0, -200)$ with $\beta = 0$

$$|H| = -3600x_1^2 + 6400x_1 + 400x_2 - 3402 = -602.$$

Furthermore,

$$H_{\mathbf{xx}}^* = \frac{\partial^2 L(\mathbf{x}^*, \lambda^*)}{\partial \mathbf{x}^2} = \begin{bmatrix} 802 & -400 \\ -400 & 200 \end{bmatrix}$$

has $|H_{\mathbf{xx}}^*| = 400$ and is positive definite. However, $L(\mathbf{x}^*, \lambda) = L(\mathbf{x}^*, \lambda^*) \forall \lambda$, since $\psi(\mathbf{x}^*) = \mathbf{0}$. Thus $(\mathbf{x}^*, \lambda^*)$ is not a *proper* saddle point, since $H_{\lambda\lambda} = \partial^2 L / \partial \lambda^2 \equiv 0$ instead of $H_{\lambda\lambda} < 0$. However, at \mathbf{y}^* with $\beta = 0$

$$\mathcal{H}^*|_{\beta=0} = \begin{bmatrix} \frac{\partial^2 L}{\partial x_1^2} & \frac{\partial^2 L}{\partial x_1 \partial x_2} & -\frac{\partial \psi}{\partial x_1} \\ \frac{\partial^2 L}{\partial x_1 \partial x_2} & \frac{\partial^2 L}{\partial x_2^2} & -\frac{\partial \psi}{\partial x_2} \\ -\frac{\partial \psi}{\partial x_1} & -\frac{\partial \psi}{\partial x_2} & 0 \end{bmatrix}_{\mathbf{y}^*_{\beta=0}} = \begin{bmatrix} 802 & -400 & 2 \\ -400 & 200 & -1 \\ 2 & -1 & 0 \end{bmatrix}$$

is indefinite, with $|\mathcal{H}^*|_{\beta=0} = -2 \neq 0$. Thus \mathbf{x}^* is a “nonsingular” point [13], so there exists $\beta \geq 0$ such that $\mathcal{H}_{\mathbf{xx}}^* = \partial^2 \mathcal{L}(\mathbf{x}^*, \lambda^*) / \partial \mathbf{x}^2$ is positive definite. In our case $\beta = 0$ suffices, since $H_{\mathbf{xx}}^*$ is already positive definite.

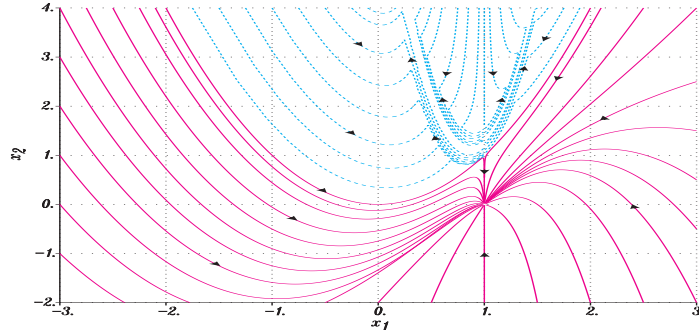


Figure 14: Newton's method ($\lambda(0) = 0$, $\beta = 0$).

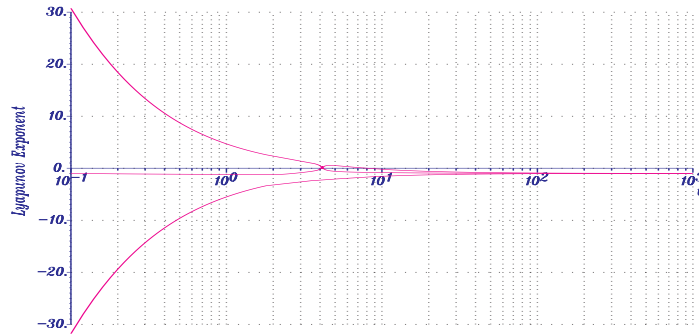


Figure 15: Lyapunov exponents for Newton's method on L .

Figure 14 shows trajectories for Newton's method for $\lambda(0) = 0$ and $\beta = 0$. All of the solid trajectories, generated with standard 4-th order Runge-Kutta with fixed step size $\Delta t = 2 \times 10^{-3}$, rapidly converge to $(x_1^*, x_2^*, \lambda^*) = (1, 0, -200)$. The dashed trajectories all reach points where $|\mathcal{H}| = 0$ and do not converge to the constrained minimal point. These trajectories were generated using Branin's method [5], [6], in which $|\mathcal{H}| = 0$ problems are avoided by replacing \mathcal{H}^{-1} in (83) with $\text{adj}(\mathcal{H})$ from (85). The resulting $[\mathbf{x}(t), \lambda(t)]$ trajectories are the same as for Newton's method except for the plot speed and the direction of motion when $|\mathcal{H}| = 0$ surfaces are "crossed".

Figure 15 shows the Lyapunov exponent time histories for Newton's method applied to L , starting from $(x_1, x_2, \lambda) = (-2.5, 0, 0)$ with $\beta = 0$. The system is initially moderately stiff but achieves $\Sigma(t) = |\sigma_{\max}(t) - \sigma_{\min}(t)| < 10$ in approximately 1 sec., with $\Sigma(t) \rightarrow 0$ as all of the Lyapunov exponents converge to $\sigma_k = -1$.

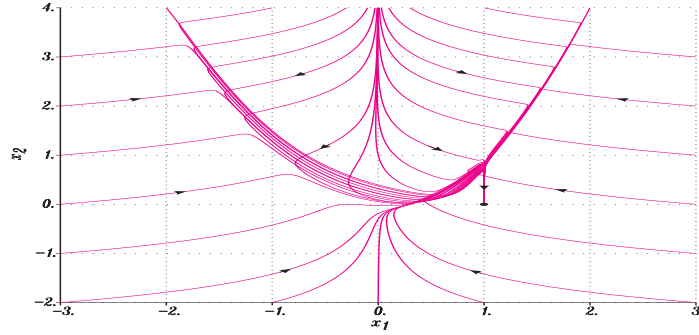


Figure 16: Gradient Enhanced Min-Max ($\lambda(0) = 0, \beta = 0$).

9.4 Gradient enhanced min-max

For GEMM applied to our Example problem of Rosenbrock’s function with a parabolic constraint, we have from (44)

$$\mathcal{F} = \begin{bmatrix} \gamma_x \|\mathbf{h}\| + \mathcal{H}_{11} & \mathcal{H}_{12} & -2(x_1 - 2) \\ \mathcal{H}_{21} & \gamma_x \|\mathbf{h}\| + \mathcal{H}_{22} & -1 \\ -2(x_1 - 2) & -1 & -\gamma_\lambda \|\mathbf{h}\| \end{bmatrix},$$

where

$$\mathcal{H} = [\mathcal{H}_{ij}] = \begin{bmatrix} \mathcal{H}_{11} & -400x_1 + 2\beta(x_1 - 2) & -2(x_1 - 2) \\ -400x_1 + 2\beta(x_1 - 2) & 200 + \beta & -1 \\ -2(x_1 - 2) & -1 & 0 \end{bmatrix},$$

$$\mathbf{h} = \nabla_{\mathbf{y}} \mathcal{L} = \begin{bmatrix} 400(x_1^2 - x_2)x_1 - 2(1 - x_1) + \left(\beta \left[(x_1 - 2)^2 + (x_2 - 1)\right] - \lambda\right) 2(x_1 - 2) \\ -200(x_1^2 - x_2) + \left(\beta \left[(x_1 - 2)^2 + (x_2 - 1)\right] - \lambda\right) \\ -(x_1 - 2)^2 - x_2 + 1 \end{bmatrix}$$

with $\mathcal{H}_{11} = 1200x_1^2 - 400x_2 + 2 + 4\beta(x_1 - 2)^2 + 2\left(\beta \left[(x_1 - 2)^2 + (x_2 - 1)\right] - \lambda\right)$.

From Theorem 7.2, for $\mathbf{y} \neq \mathbf{y}^*$ and $\gamma_\lambda > 0$, we have $|\mathcal{F}| < 0$ provided $\gamma_x > 0$ is sufficiently large so that $\gamma_x \|\mathbf{h}\| \mathbf{I}_n + \mathcal{H}_{\mathbf{x}\mathbf{x}}$ is positive definite for all $\mathbf{y} \neq \mathbf{y}^*$. We choose $\gamma_x = 10$ and $\gamma_\lambda = 0.1$. For our Example system Figure 16 shows Gradient Enhanced Min-Max (GEMM) trajectories applied to the Lagrangian L with step size $\Delta t = 1$. Figure 17 shows Gradient Enhanced Min-Max trajectories applied to the augmented Lagrangian \mathcal{L} , with $\beta = 5$ and step size $\Delta t = 1$.

Figure 18 shows the Lyapunov exponent time histories for GEMM applied to L , starting from $(x_1, x_2, \lambda) = (-2.5, 0, 0)$ with $\beta = 0, \gamma_x = 10$, and $\gamma_\lambda = 0.1$. The system is uniformly non stiff, with $\max \Sigma(t) < 1$ and $\Sigma(t) \rightarrow 0$ as all of the Lyapunov exponents converge to $\sigma_k = -1$.

10 Constrained Trajectory Following Performance

For each Gradient Transformation algorithm in Section 4 simulation experiments were conducted for a variety of parameter combinations, with the algorithms being applied to

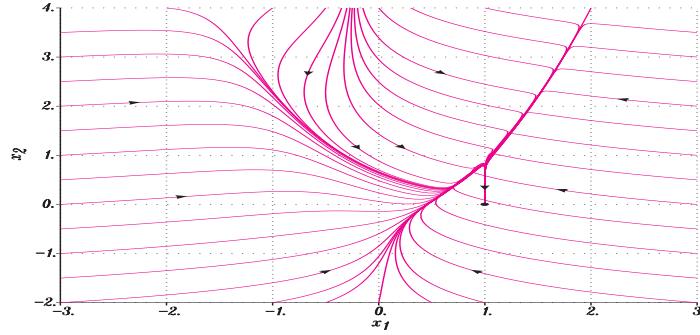


Figure 17: Gradient Enhanced Min-Max ($\lambda(0) = 0$, $\beta = 5$).

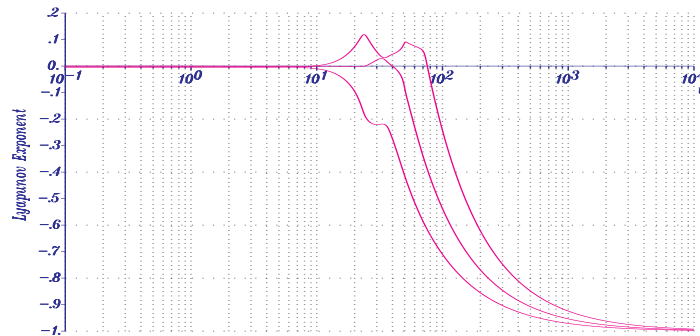


Figure 18: Lyapunov exponents for GEMM on L .

both the Lagrangian L and the augmented Lagrangian \mathcal{L} . Table 3 shows the parameter values for each Gradient Transformation trajectory following method that we studied. For comparison, all trajectories were started at a point $\mathbf{x}(0) = (-2.5, 0)$ from which all the algorithms converged to the constrained minimal point $\mathbf{y}^* = (1, 0, -200)$.

Table 4 shows step sizes and simulation results for the methods in Table 3. For each algorithm a trajectory $\mathbf{y}(t)$ was computed starting from $\mathbf{x}(0) = (-2.5, 0)$ using standard 4-*th* order Runge–Kutta with fixed step size Δt , determined to control the approximate initial single step displacement $\Delta s = \|\mathbf{y}(\Delta t) - \mathbf{y}(0)\|$. The trajectories were terminated when $\|\nabla_{\mathbf{y}}\mathcal{L}\| \leq 10^{-3}$. For reference, we include results for Min-Max Ascent starting with $\lambda(0) = \lambda^*$, which yields fairly fast convergence to \mathbf{y}^* . All other simulations were started with $\lambda(0) = 0$.

11 Summary

For the problem of minimizing a scalar-valued function subject to equality constraints, the Gradient Transformation family of differential equation algorithms includes, as special cases: Min-Max Ascent, Newton’s method, Hestenes’ Method of Multipliers, and a Gradient Enhanced Min-Max (GEMM) algorithm extended to handle equality constraints. Applied to Rosenbrock’s function with a parabolic constraint, we find that

Table 3: Gradient Transformation algorithm parameters.

Method	$\lambda(0)$	β	γ_x	γ_λ
Min-Max L	0	0	0	0
Min-Max L^*	-200	0	0	0
Hestenes \mathcal{L}_1	0	5	0	0
Hestenes \mathcal{L}_2	0	100	0	0
Newton L	0	0	0	0
Newton \mathcal{L}_1	0	5	0	0
Newton \mathcal{L}_2	0	100	0	0
GEMM L	0	0	10	0.1
GEMM \mathcal{L}_1	0	5	10	0.1
GEMM \mathcal{L}_2	0	100	10	0.1

Table 4: Simulation results for Gradient Transformation algorithms.

Method	Speed $\ \dot{y}(0)\ $	Δt	$\ y(\Delta t) - y(0)\ $	Final t	# Steps	Ratio
Min-Max L	6.381×10^3	2×10^{-4}	0.747	1380.364	6901820	92024
Min-Max L^*	8.125×10^3	1×10^{-4}	0.590	0.095	950	13
Hestenes \mathcal{L}_1	8.060×10^3	1×10^{-4}	0.568	288.016	2880161	38402
Hestenes \mathcal{L}_2	4.104×10^4	2×10^{-5}	0.630	24.965	1248253	16643
Newton L	3.055×10^2	2×10^{-3}	0.610	15.670	7835	104
Newton \mathcal{L}_1	3.494×10^2	2×10^{-3}	0.698	15.904	7952	106
Newton \mathcal{L}_2	1.053×10^3	5×10^{-4}	0.526	17.529	35058	467
GEMM L	9.394×10^{-2}	1	0.094	75	75	1
GEMM \mathcal{L}_1	9.303×10^{-2}	1	0.093	75	75	1
GEMM \mathcal{L}_2	9.300×10^{-2}	1	0.093	78	78	1

Min-Max Ascent is globally asymptotically stable but very stiff and has very slow convergence. Hestenes’ Method of Multipliers is also globally asymptotically stable and has faster convergence, but is still very slow and very stiff. Newton’s method is not stiff, but does not yield global asymptotic stability. However, GEMM is both globally asymptotically stable and not stiff. The stiffness of the Gradient Transformation family is studied in terms of Lyapunov exponent time histories. Starting from points where all the methods in this paper do work, we show that Min-Max Ascent and Hestenes’ Method of Multipliers are very stiff and slow to converge, but with the Method of Multipliers being approximately 2 times as fast as Min-Max Ascent. Newton’s method, where it works, is not stiff and is approximately 900 times as fast as Min-Max Ascent and 400 times as fast as the Method of Multipliers. In contrast, the Gradient Enhanced Min-Max method is globally convergent, is not stiff, and is approximately 100 times faster than Newton’s method, 40,000 times faster than the Method of Multipliers, and 90,000 times faster than Min-Max Ascent

References

[1] Vincent, T. L. and Grantham, W. J. Trajectory Following Methods in Control System Design. *J. of Global Optimization* **23** (2002) 267–282.

[2] Goh, B. S. Algorithms for Unconstrained Optimization Problems Via Control Theory. *J. of Optimization Theory and Applications* **92** (3) (1997) 581–604.

[3] Arrow, K. J., Hurwicz, L., and Uzawa, H. *Studies in Linear and Non-Linear Programming*. Stanford Univ. Press, Stanford, California, 1958.

- [4] Vincent, T. L., Goh, B. S., and Teo, K. L. Trajectory-Following Algorithms for Min-Max Optimization Problems. *J. of Optimization Theory and Applications* (75) (3) (1992) 501–519.
- [5] Gomulka, J. Remarks on Branin’s Method for Solving Nonlinear Equations. *Towards Global Optimization* (L. C. W. Dixon and G. P. Szegö, eds.). North-Holland, Amsterdam, 1972, pp. 96–106.
- [6] Gomulka, J. Two Implementations of Branin’s Method: Numerical Experience. *Towards Global Optimization 2* (L. C. W. Dixon and G. P. Szegö, eds.). North-Holland, Amsterdam, 1978, pp. 151–164.
- [7] Grantham, W. J. Trajectory Following Optimization by Gradient Transformation Differential Equations. In: *Proc. 42nd I.E.E.E. Conf. on Decision and Control*. Maui, HI, December 2003, pp. 5496–5501.
- [8] Grantham, W. J. Gradient Transformation Trajectory Following Algorithms for Determining Stationary Min-Max Saddle Points. *Advances in Dynamic Game Theory and Applications* (S. J. Jørgensen, T. L. Vincent and M. Quincampoix, eds.). Birkhäuser, Boston, 2006.
- [9] Vincent, T. L. and Grantham, W. J. *Optimality in Parametric Systems*. Wiley-Interscience, New York., 1981.
- [10] Fletcher, R. *Practical Methods of Optimization*. Wiley, New York, 1987.
- [11] Bertsekas, D. P. Multiplier Methods: A Survey. *Automatica* **12** (2) (1976) 133–145.
- [12] Bertsekas, D. P. *Constrained Optimization and Lagrange Multiplier Methods*. Athene Scientific, Belmont, MA, 1996.
- [13] Hestenes, M. R. Multiplier and Gradient Methods. *J. of Optimization Theory and Applications* **4** (1969) 303–320.
- [14] Vincent, T. and Grantham, W. *Nonlinear and Optimal Control Systems*. Wiley, New York, 1997.
- [15] Grantham, W. J. and Lee, B. S. A Chaotic Limit Cycle Paradox. *Dynamics and Control* **3** (2) (1993) 159–173.
- [16] Wolf, A., Swift, J. B., Swinney, H. L., and Vastano, J. A. Determining Lyapunov Exponents from a Time Series. *Physica 16D* (1985) 285–317.
- [17] Chong, E. K. P. and Zak, S. H. *An Introduction to Optimization*. Wiley, New York, 2nd ed., 2001.
- [18] Goh, B. S. Greatest Descent Algorithms in Unconstrained Optimization. *J. of Optimization Theory and Applications* **142** (2009) 275–289.
- [19] Luenberger, D. G. *An Introduction to Dynamic Systems*. Wiley, New York, 1979.
- [20] Kato, T. *A Short Introduction to Perturbation Theory for Linear Operators*. Springer-Verlag, New York, 1982.
- [21] Brogan, W. *Modern Control Theory*, Prentice-Hall, Englewood Cliffs, 1982.